

Thymic stromal lymphopoietin–elicited basophil responses promote eosinophilic esophagitis

Mario Noti^{1,2,27}, Elia D Tait Wojno^{1,2,27}, Brian S Kim^{1–3}, Mark C Siracusa^{1,2}, Paul R Giacomini^{1,2,4}, Meera G Nair^{1,2,5}, Alain J Benitez⁶, Kathryn R Ruymann⁷, Amanda B Muir⁶, David A Hill^{1,2,7}, Kudakwashe R Chikwava⁸, Amin E Moghaddam⁹, Quentin J Sattentau⁹, Aneesh Alex^{10–12}, Chao Zhou^{10–12}, Jennifer H Yearley¹³, Paul Menard-Katcher¹⁴, Masato Kubo^{15,16}, Kazushige Obata-Ninomiya^{17,18}, Hajime Karasuyama^{17,18}, Michael R Comeau¹⁹, Terri Brown-Whitehorn⁷, Rene de Waal Malefyt²⁰, Patrick M Sleiman^{21–23}, Hakon Hakonarson^{21–23}, Antonella Cianferoni⁷, Gary W Falk^{14,24,25}, Mei-Lun Wang^{6,24,25}, Jonathan M Spergel^{2,7,24,25} & David Artis^{1,2,24–26}

Eosinophilic esophagitis (EoE) is a food allergy–associated inflammatory disease characterized by esophageal eosinophilia. Current management strategies for EoE are nonspecific, and thus there is a need to identify specific immunological pathways that could be targeted to treat this disease. EoE is associated with polymorphisms in the gene that encodes thymic stromal lymphopoietin (TSLP), a cytokine that promotes allergic inflammation, but how TSLP might contribute to EoE disease pathogenesis has been unclear. Here, we describe a new mouse model of EoE-like disease that developed independently of IgE, but was dependent on TSLP and basophils, as targeting TSLP or basophils during the sensitization phase limited disease. Notably, therapeutic TSLP neutralization or basophil depletion also ameliorated established EoE-like disease. In human subjects with EoE, we observed elevated *TSLP* expression and exaggerated basophil responses in esophageal biopsies, and a gain-of-function *TSLP* polymorphism was associated with increased basophil responses in patients with EoE. Together, these data suggest that the TSLP–basophil axis contributes to the pathogenesis of EoE and could be therapeutically targeted to treat this disease.

EoE is a food allergy–associated inflammatory disease that affects children and adults^{1–3}. In industrialized countries, the incidence of EoE has increased dramatically in the past 30 years, resulting in a considerable public health and economic burden^{2,4,5}. EoE is characterized by esophageal eosinophilia and inflammation and histological changes in the esophagus associated with stricture, dysphagia and food impaction^{1–3}. Currently, treatment strategies for EoE are nonspecific and impose a burden on patients. Although swallowed topical steroids can be effective in

limiting EoE-associated inflammation, there are concerns regarding the long-term use of steroids, particularly in children^{2,6}. Adherence to an elemental diet that eliminates exposure to foods that trigger EoE results in resolution of symptoms in many patients; however, this approach requires disruptive changes in lifestyle and eating habits^{2,6,7}. Thus, there is a need to identify new drug targets and more specific therapies⁷. The observations that immune suppression or removal of dietary trigger foods can ameliorate EoE symptoms indicate that EoE is a food antigen–driven

¹Department of Microbiology, Perelman School of Medicine, University of Pennsylvania, Philadelphia, Pennsylvania, USA. ²Institute for Immunology, Perelman School of Medicine, University of Pennsylvania, Philadelphia, Pennsylvania, USA. ³Department of Dermatology, Perelman School of Medicine, University of Pennsylvania, Philadelphia, Pennsylvania, USA. ⁴Centre for Biodiscovery and Molecular Development of Therapeutics, Queensland Tropical Health Alliance, James Cook University, Cairns, Queensland, Australia. ⁵Division of Biomedical Sciences, School of Medicine, University of California–Riverside, Riverside, California, USA. ⁶Division of Gastroenterology, Hepatology and Nutrition, Children’s Hospital of Philadelphia, Philadelphia, Pennsylvania, USA. ⁷Department of Pediatrics, Division of Allergy and Immunology, Children’s Hospital of Philadelphia, Philadelphia, Pennsylvania, USA. ⁸Department of Pathology and Laboratory Medicine, Children’s Hospital of Philadelphia, Philadelphia, Pennsylvania, USA. ⁹The Sir William Dunn School of Pathology, The University of Oxford, Oxford, UK. ¹⁰Department of Electrical and Computer Engineering, Lehigh University, Bethlehem, Pennsylvania, USA. ¹¹Center for Photonics and Nanoelectronics, Lehigh University, Bethlehem, Pennsylvania, USA. ¹²Bioengineering Program, Lehigh University, Bethlehem, Pennsylvania, USA. ¹³Department of Pathology, Merck Research Laboratories, Palo Alto, California, USA. ¹⁴Division of Gastroenterology, Perelman School of Medicine, University of Pennsylvania, Philadelphia, Pennsylvania, USA. ¹⁵Laboratory for Cytokine Regulation, Research Center for Integrative Medical Science, RIKEN Yokohama Institute, Kanagawa, Japan. ¹⁶Division of Molecular Pathology, Research Institute for Biomedical Science, Tokyo University of Science, Chiba, Japan. ¹⁷Department of Immune Regulation, Tokyo Medical and Dental University Graduate School, Tokyo, Japan. ¹⁸Japan Science and Technology Agency, Core Research for Evolutionary Science and Technology, Tokyo Medical and Dental University Graduate School, Tokyo, Japan. ¹⁹Inflammation Research, Amgen, Seattle, Washington, USA. ²⁰Therapeutic Area Biology and Pharmacology, Merck Research Laboratories, Palo Alto, California, USA. ²¹Center for Applied Genomics, Abramson Research Center, Children’s Hospital of Philadelphia, Philadelphia, Pennsylvania, USA. ²²Division of Human Genetics, Abramson Research Center, Children’s Hospital of Philadelphia, Philadelphia, Pennsylvania, USA. ²³Department of Pediatrics, Perelman School of Medicine, University of Pennsylvania, Philadelphia, Pennsylvania, USA. ²⁴Joint Penn–Children’s Hospital of Philadelphia Center for Digestive, Liver and Pancreatic Medicine, Perelman School of Medicine, University of Pennsylvania and Children’s Hospital of Philadelphia, Philadelphia, Pennsylvania, USA. ²⁵Center for Molecular Studies in Digestive and Liver Diseases, Department of Medicine, Division of Gastroenterology, Perelman School of Medicine, University of Pennsylvania, Philadelphia, Pennsylvania, USA. ²⁶Department of Pathobiology, School of Veterinary Medicine, University of Pennsylvania, Philadelphia, Pennsylvania, USA. ²⁷These authors contributed equally to this work. Correspondence should be addressed to D.A. (dartis@mail.med.upenn.edu).

Received 18 March; accepted 18 June; published online 21 July 2013; doi:10.1038/nm.3281

disease mediated by aberrant immune responses^{1,2,8}. Therefore, targeting the dysregulated immunological pathways that underlie EoE could offer new treatment strategies for this disease.

Studies investigating the immunological mechanisms that mediate EoE have shown that various immune cell types, including eosinophils, mast cells, type 2 helper T (T_H2) cells that produce interleukin-4 (IL-4), IL-5, and IL-13, and IgE-producing B cells, may contribute to esophageal inflammation during EoE^{1–3,9}. Further, recent work has shown that there is a strong association between a gain-of-function polymorphism in the gene that encodes the predominantly epithelial cell-derived cytokine TSLP and the development of EoE in children^{10,11}. TSLP is associated with multiple allergic disorders^{10–16} and is thought to promote allergic inflammation by activating dendritic cells, inducing T_H2 cell responses, supporting IgE production and eliciting the population expansion of phenotypically and functionally distinct basophils^{12,17–21}. However, whether TSLP directly promotes inflammatory responses associated with EoE and the mechanisms by which polymorphisms in *TSLP* and increased TSLP expression may contribute to the pathogenesis of EoE in patients has been unknown.

RESULTS

A new mouse model of experimental EoE-like disease

To investigate whether TSLP directly promotes EoE disease pathogenesis, we developed a new mouse model of EoE-like disease that

is associated with exaggerated TSLP production. Multiple studies in mouse models and humans suggest that sensitization to food allergens may occur at sites where the skin barrier is disrupted, such as atopic dermatitis lesions^{22–24}. Thus, we employed a model in which mice were epicutaneously sensitized to a food antigen, ovalbumin (OVA), on a developing atopic dermatitis-like skin lesion induced by topical treatment with the vitamin D analog MC903 (Fig. 1a). Consistent with previous reports^{17,25–27}, wild-type (WT) BALB/c mice treated epicutaneously with the vitamin D analog MC903 showed increased TSLP expression in the skin compared to ethanol vehicle-treated control mice (Fig. 1b). Epicutaneous sensitization to and subsequent oral challenge with OVA resulted in the development of experimental EoE-like disease that was characterized by inflammation, edema and eosinophilia in the esophagus, as measured histologically and quantified by enumeration of eosinophils per high-power field (HPF) (Fig. 1c,d). Flow cytometric analysis (Fig. 1e,f) and immunofluorescence staining (Fig. 1g) also demonstrated that there was an accumulation of eosinophils in esophageal tissues of mice with EoE-like disease, and electron microscopic (EM) analysis revealed the presence of degranulated eosinophils in these tissues (Fig. 1h). We also observed significantly higher expression of genes that encode T_H2 cytokines and the basophil-specific protease *Mcpt8* and a trend toward increased *Tslp* expression in esophageal tissues of mice with EoE-like disease compared to control mice (Fig. 1i). Further, we observed a similar

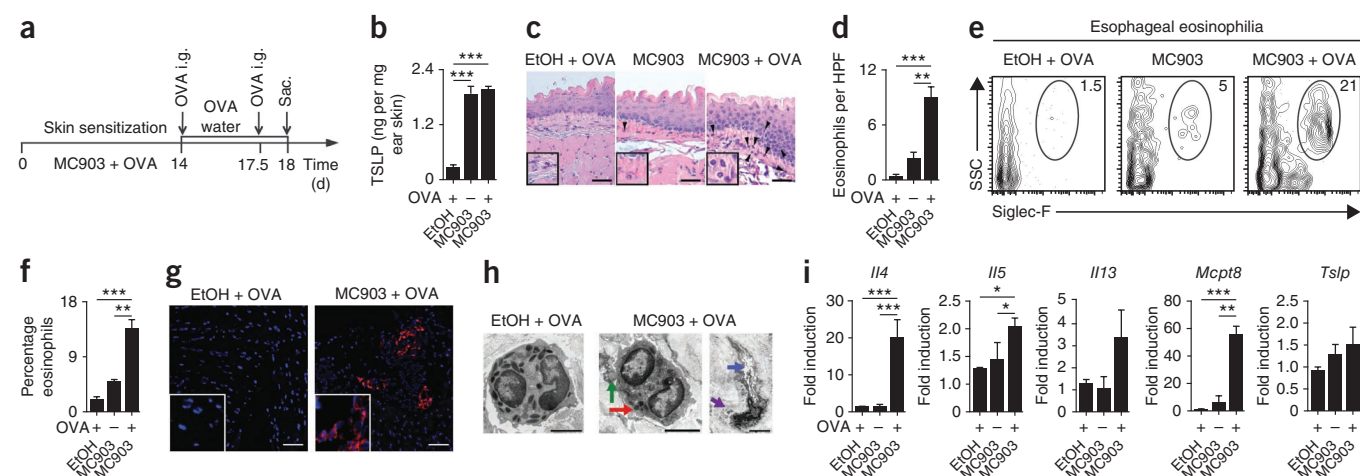


Figure 1 Experimental mouse model of EoE-like disease. (a) Schematic of EoE-like disease mouse model in which WT BALB/c mice are epicutaneously sensitized for 14 d with OVA on a developing atopic dermatitis-like skin lesion, challenged intragastrically (i.g.) with OVA on days 14 and 17.5 and sacrificed (sac.) at day 18. (b) TSLP (ng per mg of ear skin) expression in supernatants of overnight-cultured skin (ears) measured by ELISA. Data are from one experiment (EtOH + OVA, $n = 3$; MC903, $n = 3$; MC903 + OVA, $n = 4$) and are representative of three independent replicates. EtOH, ethanol. (c) Histological sections (H&E staining) from the esophagus. Arrowheads identify tissue-infiltrating eosinophils. Scale bar, 25 μ m. Insets: $\times 4$ magnification of whole image focusing on eosinophils. (d) Number of eosinophils per HPF in the esophagus. (e) Representative flow cytometry plots showing frequencies of eosinophils in esophageal tissues. Data in c–e are from one experiment (EtOH + OVA, $n = 3$; MC903, $n = 3$; MC903 + OVA, $n = 4$) and are representative of three or more independent replicates. (f) Frequencies of eosinophils in esophageal tissues, as measured by flow cytometry. Data are from three pooled experiments (EtOH + OVA, $n = 7$; MC903, $n = 8$; MC903 + OVA, $n = 11$). (g) Immunofluorescence staining for eosinophils (Siglec-F-specific mAb, red) in esophageal tissues. Counterstaining with DAPI (blue). Scale bar, 25 μ m. Images are representative of two controls and three EoE-like disease samples. Insets: $\times 4$ magnification of whole image focusing on eosinophils. (h) Representative EM image of an eosinophil in the esophagus of control mice with intact granules with electron dense cores (left) or degranulating eosinophils in MC903 + OVA-treated mice (right), showing loss of electron density in granule cores (red arrow), granule extrusion channels (blue arrow) and complete loss of granule contents (green arrow) into the extracellular matrix (purple arrow). Scale bar, 2 μ m. (i) mRNA expression of T_H2 cytokines (*Il4*, *Il5*, *Il13*), the basophil-specific protease *Mcpt8* and *Tslp* in the esophagus. Data depicted are from one experiment (EtOH + OVA, $n = 3$; MC903, $n = 3$; MC903 + OVA, $n = 4$) and are representative of three independent replicates. y axis shows fold induction compared to controls (see Online Methods). (j) Representative images of esophagi, with incidence of impaction. Arrowheads identify impacted food. Data depicted are from two pooled experiments (EtOH + OVA, $n = 7$; MC903 + OVA, $n = 9$). All parameters were assessed 12 h post-final oral antigen challenge. Data in a–i are from mice challenged twice with OVA, and data in j are from mice challenged six times with OVA. Results are shown as mean \pm s.e.m., and a nonparametric, one-way Kruskal-Wallis analysis of variance (ANOVA) with Dunn's *post hoc* testing was used to determine significance. * $P \leq 0.05$; ** $P \leq 0.01$; *** $P \leq 0.001$.

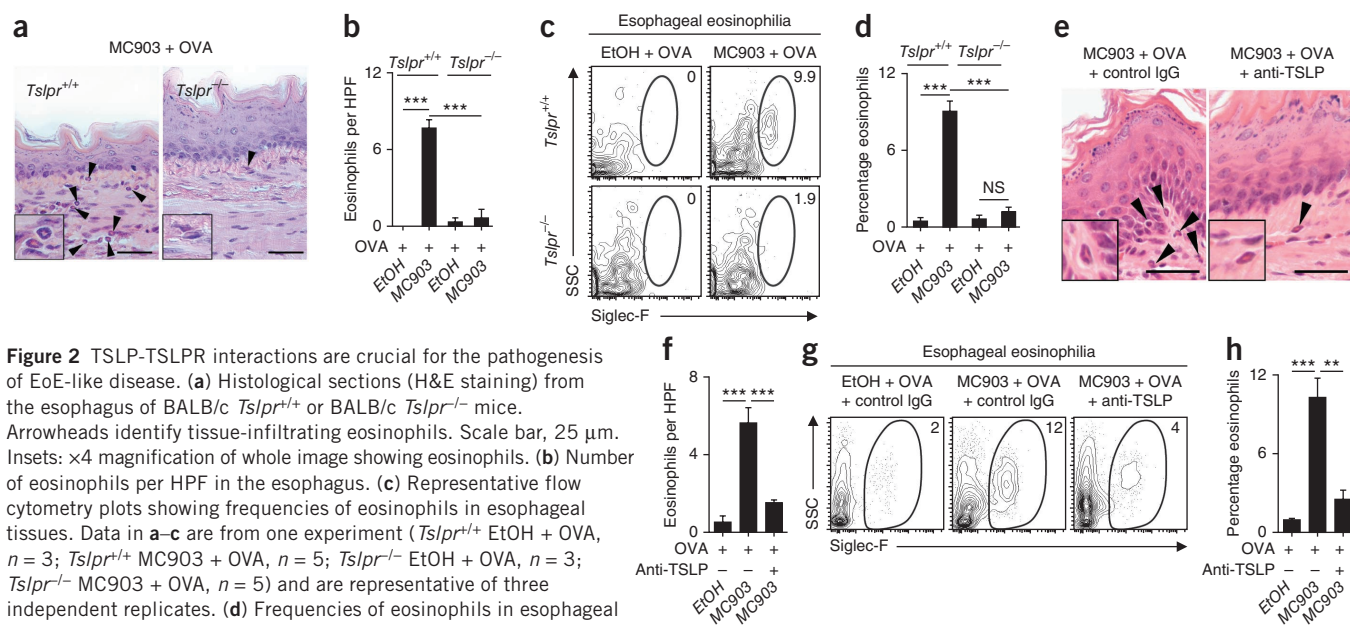


Figure 2 TSLP-TSLPR interactions are crucial for the pathogenesis of EoE-like disease. **(a)** Histological sections (H&E staining) from the esophagus of BALB/c *Tslpr*^{+/+} or BALB/c *Tslpr*^{-/-} mice. Arrowheads identify tissue-infiltrating eosinophils. Scale bar, 25 μ m. Insets: $\times 4$ magnification of whole image showing eosinophils. **(b)** Number of eosinophils per HPF in the esophagus. **(c)** Representative flow cytometry plots showing frequencies of eosinophils in esophageal tissues. Data in **a–c** are from one experiment (*Tslpr*^{+/+} EtOH + OVA, $n = 3$; *Tslpr*^{+/+} MC903 + OVA, $n = 5$; *Tslpr*^{-/-} EtOH + OVA, $n = 3$; *Tslpr*^{-/-} MC903 + OVA, $n = 5$) and are representative of three independent replicates. **(d)** Frequencies of eosinophils in esophageal tissues, as measured by flow cytometry. Data are from three pooled experiments (*Tslpr*^{+/+} EtOH + OVA, $n = 5$; *Tslpr*^{+/+} MC903 + OVA, $n = 11$; *Tslpr*^{-/-} EtOH + OVA, $n = 5$; *Tslpr*^{-/-} MC903 + OVA, $n = 12$). **(e)** Histological sections (H&E staining) from the esophagus of WT BALB/c mice treated with an isotype control or TSLP-specific mAb (anti-TSLP). Arrowheads identify tissue-infiltrating eosinophils. Scale bar, 50 μ m. Insets: $\times 4$ magnification of whole image showing eosinophils. **(f)** Number of eosinophils per HPF in the esophagus. **(g)** Representative flow cytometry plots showing frequencies of eosinophils in esophageal tissues. Data in **e–g** are from one experiment (EtOH + OVA + IgG, $n = 3$; MC903 + OVA + IgG, $n = 3$; MC903 + OVA + anti-TSLP mAb, $n = 3$) and are representative of three independent replicates. **(h)** Frequencies of eosinophils in esophageal tissues, as measured by flow cytometry. Data are from three pooled experiments (EtOH + OVA + IgG, $n = 5$; MC903 + OVA + IgG, $n = 9$; MC903 + OVA + anti-TSLP mAb, $n = 10$). All parameters were assessed 12 h after final oral antigen challenge. Data are from mice challenged twice with OVA. Results are shown as mean \pm s.e.m., and a nonparametric, one-way Kruskal-Wallis ANOVA with Dunn's *post hoc* testing or a nonparametric, two-way ANOVA with Bonferroni's *post hoc* testing were used to determine significance. ** $P \leq 0.01$; *** $P \leq 0.001$. NS, not significant.

pattern of EoE-like disease in mice that were epicutaneously sensitized to crude peanut extract (CPE) on an atopic dermatitis-like skin lesion (**Supplementary Fig. 1a–c**), confirming that sensitization to a natural food allergen in the presence of elevated amounts of TSLP results in experimental EoE-like disease. Eosinophil accumulation in this model was not restricted to the esophagus, as mice with EoE-like disease also showed eosinophilia in the gastrointestinal tract after epicutaneous sensitization and oral challenge with OVA (**Supplementary Fig. 1d,e**) associated with antigen-specific T_H2 cytokine responses in the mesenteric lymph node and spleen (**Supplementary Fig. 1f,g**).

EoE in humans is diagnosed on the basis of immunological parameters and the presence of physiological changes in esophageal tissue and signs of esophageal dysfunction, including food impaction, which occurs in approximately 40% of patients with EoE^{1–3,28}. To assess whether clinical manifestations of EoE were present in the experimental mouse model of EoE-like disease, we challenged mice that had existing EoE-like disease repeatedly with OVA to induce prolonged esophageal inflammation. Although analysis using optical coherence tomography (OCT), which allows for high-resolution imaging of live biological tissues based on optical scattering^{29,30}, revealed that EoE-like disease was characterized by minimal changes in the thickness of the esophageal epithelium, (**Supplementary Fig. 2a,b**), prolonged esophageal inflammation was associated with food impaction in the esophagus. Approximately 30% of fasted mice with EoE-like disease exhibited food impaction at the time of killing, but we never observed food impaction in the esophagus of control (ethanol)-treated mice (**Fig. 1j**). Collectively, these data indicate that this new model of EoE-like disease is characterized by a number of immunological

and pathophysiological changes in esophageal tissues and signs of esophageal dysfunction similar to those observed in humans with EoE^{1–3,31–34}.

EoE-like disease is dependent on TSLP but independent of IgE

To determine whether TSLP directly promotes the pathogenesis of experimental EoE-like disease in mice, we epicutaneously sensitized WT BALB/c (*Tslpr*^{+/+}) mice or mice deficient in the TSLP receptor (TSLPR) (*Tslpr*^{-/-}) to OVA followed by oral antigen challenge (see **Fig. 1a**). Whereas sensitized and challenged *Tslpr*^{+/+} mice showed esophageal eosinophilia and associated inflammation, *Tslpr*^{-/-} mice did not develop esophageal eosinophilia (**Fig. 2a–d**). Using an alternative approach to abrogate TSLP signaling, we found that multiple systemic treatments with a monoclonal antibody (mAb) that neutralizes TSLP during epicutaneous sensitization with OVA in WT BALB/c mice also limited eosinophil infiltration in the esophagus after oral challenge (**Fig. 2e–h**).

To test whether TSLP was sufficient for the development of EoE-like disease during epicutaneous sensitization, we intradermally injected mice with exogenous recombinant TSLP (rTSLP) in the presence or absence of OVA and challenged them orally (**Supplementary Fig. 3a**). Mice sensitized to OVA in the presence of rTSLP also showed esophageal eosinophilia after oral challenge compared to mice treated with OVA alone or rTSLP alone (**Supplementary Fig. 3b**). In a complementary approach, *Tslpr*^{+/+} mice were treated with control antibody or a TSLP-specific mAb, and *Tslpr*^{-/-} mice were sensitized with OVA on tape-stripped skin (**Supplementary Fig. 3c**). Tape-stripping was associated with elevated local TSLP production following physical

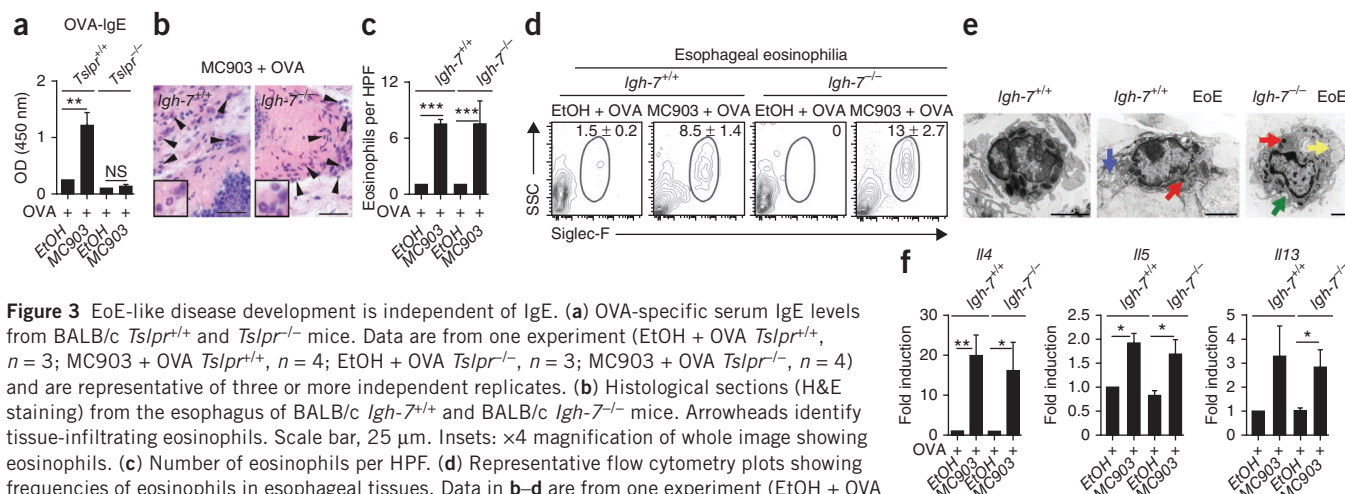


Figure 3 EoE-like disease development is independent of IgE. **(a)** OVA-specific serum IgE levels from BALB/c *Tslpr*^{+/+} and *Tslpr*^{-/-} mice. Data are from one experiment (EtOH + OVA *Tslpr*^{+/+}, *n* = 3; MC903 + OVA *Tslpr*^{+/+}, *n* = 4; EtOH + OVA *Tslpr*^{-/-}, *n* = 3; MC903 + OVA *Tslpr*^{-/-}, *n* = 4) and are representative of three or more independent replicates. **(b)** Histological sections (H&E staining) from the esophagus of BALB/c *Igh*-7^{+/+} and BALB/c *Igh*-7^{-/-} mice. Arrowheads identify tissue-infiltrating eosinophils. Scale bar, 25 μ m. Insets: \times 4 magnification of whole image showing eosinophils. **(c)** Number of eosinophils per HPF. **(d)** Representative flow cytometry plots showing frequencies of eosinophils in esophageal tissues. Data in **b–d** are from one experiment (EtOH + OVA *Igh*-7^{+/+}, *n* = 3; MC903 + OVA *Igh*-7^{+/+}, *n* = 3; EtOH + OVA *Igh*-7^{-/-}, *n* = 3; MC903 + OVA *Igh*-7^{-/-}, *n* = 4) and are representative of three or more independent replicates. **(e)** Representative EM image of an eosinophil in the esophagus of control *Igh*-7^{+/+} mice with intact granules with electron-dense cores (left) or degranulating eosinophils in MC903 + OVA treated *Igh*-7^{+/+} (middle) or *Igh*-7^{-/-} (right) mice in various stages of degranulation, with loss of electron density in granule cores (red arrows), formation of granule extrusion channels (blue arrow), complete loss of granule contents (green arrow) and formation of lipid vesicles (yellow arrow). Scale bar, 2 μ m. **(f)** mRNA expression of Th2 cytokines in the esophagus. Data are from one experiment (EtOH + OVA *Igh*-7^{+/+}, *n* = 3; MC903 + OVA *Igh*-7^{+/+}, *n* = 3; EtOH + OVA *Igh*-7^{-/-}, *n* = 3; MC903 + OVA *Igh*-7^{-/-}, *n* = 3) and are representative of two independent replicates. y axis shows fold induction compared to controls (see Online Methods). All parameters were assessed 12 h after final oral antigen challenge. Data are from mice challenged twice with OVA. Results are shown as mean \pm s.e.m., and a nonparametric, two-way ANOVA with Bonferroni's *post hoc* testing was used to determine significance. **P* \leq 0.05, ***P* \leq 0.01; ****P* \leq 0.001. NS, not significant.

perturbation of the skin barrier (**Supplementary Fig. 3d** and ref. 35). Whereas *Tslpr*^{+/+} mice treated with control antibody that were sensitized to OVA on tape-stripped skin showed esophageal eosinophilia after oral antigen challenge, *Tslpr*^{+/+} mice treated with a TSLP-specific mAb and *Tslpr*^{-/-} mice did not develop esophageal eosinophilia (**Supplementary Fig. 3e,f**). Finally, we assessed the contribution of TSLP to the development of clinical signs of EoE-like disease. Repeated challenge with OVA following sensitization in the presence of MC903 was not associated with changes in the thickness of the esophageal epithelium. However, prolonged esophageal inflammation was associated with an increased incidence of food impaction in the esophagus in *Tslpr*^{+/+} but not *Tslpr*^{-/-} mice (**Supplementary Fig. 4a,b**). Collectively, these data indicate that TSLP-TSLPR interactions are necessary and sufficient for the development of experimental EoE-like disease in mice.

TSLP-TSLPR interactions are known to promote the production of IgE^{36,37}, a key mediator of allergic inflammation³⁸, and class-switched B cells have been observed in the esophagus of patients with EoE^{9,39,40}. In addition, MC903-induced TSLP expression was associated with high amounts of systemic OVA-specific IgE (**Fig. 3a**), suggesting that TSLP-dependent EoE-like disease in mice might be IgE dependent. To directly test this, we epicutaneously sensitized IgE-sufficient WT BALB/c (*Igh*-7^{+/+}) mice and IgE-deficient (*Igh*-7^{-/-}) mice to OVA in the presence of MC903. Following oral challenge with antigen, both *Igh*-7^{+/+} and *Igh*-7^{-/-} mice showed equivalent EoE-like disease, characterized by esophageal inflammation, elevated tissue eosinophilia (**Fig. 3b–d**), the presence of degranulated eosinophils in the esophagus (**Fig. 3e**) and significant increases in gene expression of Th2 cytokines in esophageal tissues (**Fig. 3f**). These data demonstrate that EoE-like disease can occur in an IgE-independent manner and are consistent with recent findings from clinical studies suggesting that treatment with an IgE-specific mAb does not ameliorate EoE in most patients^{41–44}. Together, these

data indicate that manipulation of the IgE pathway may not be an effective therapeutic approach for the treatment of EoE.

EoE-like disease depends on basophils

In addition to its role in promoting B cell and IgE responses, TSLP expression is associated with the selective expansion of a distinct population of basophils^{17,18}. These data suggest that basophils may contribute to TSLP-dependent, IgE-independent EoE-like disease in mice. Consistent with this hypothesis, MC903-induced expression of TSLP in the skin was associated with TSLP-dependent, IgE-independent systemic basophil responses (**Supplementary Fig. 5a,b**). To assess whether basophils contribute to the development of experimental EoE-like disease, we employed an established genetic approach to deplete basophils *in vivo*. C57BL/6 mice in which the diphtheria toxin receptor (DTR) is exclusively expressed by basophils (Baso-DTR⁺ mice)^{17,19,45} and DTR-negative littermate controls (Baso-DTR⁻ mice) were epicutaneously sensitized and orally challenged with OVA while being treated with diphtheria toxin (**Fig. 4a**). Consistent with results observed in BALB/c mice (**Fig. 1b**), we observed increased local and systemic TSLP production in C57BL/6 Baso-DTR⁻ and Baso-DTR⁺ mice sensitized to OVA in the context of MC903 treatment (data not shown). Notably, whereas Baso-DTR⁻ mice that were epicutaneously sensitized and orally challenged with OVA showed high frequencies of eosinophils in the esophagus, depletion of basophils in Baso-DTR⁺ mice (**Supplementary Fig. 5c**) led to a reduction in esophageal eosinophilia (**Fig. 4b–e**) and a reduction in expression of genes related to Th2 cytokine responses (**Supplementary Fig. 6a–c**).

Using an alternative approach, we treated epicutaneously sensitized and orally challenged WT BALB/c mice with a mAb specific for CD200R3 (Ba103) to deplete basophils⁴⁶ (**Fig. 4f**). Mice in which basophils were depleted during sensitization (**Supplementary Fig. 5d**) showed a reduced accumulation of eosinophils in the esophagus compared to control mAb-treated mice after oral challenge with OVA (**Fig. 4g–j**). Collectively, these

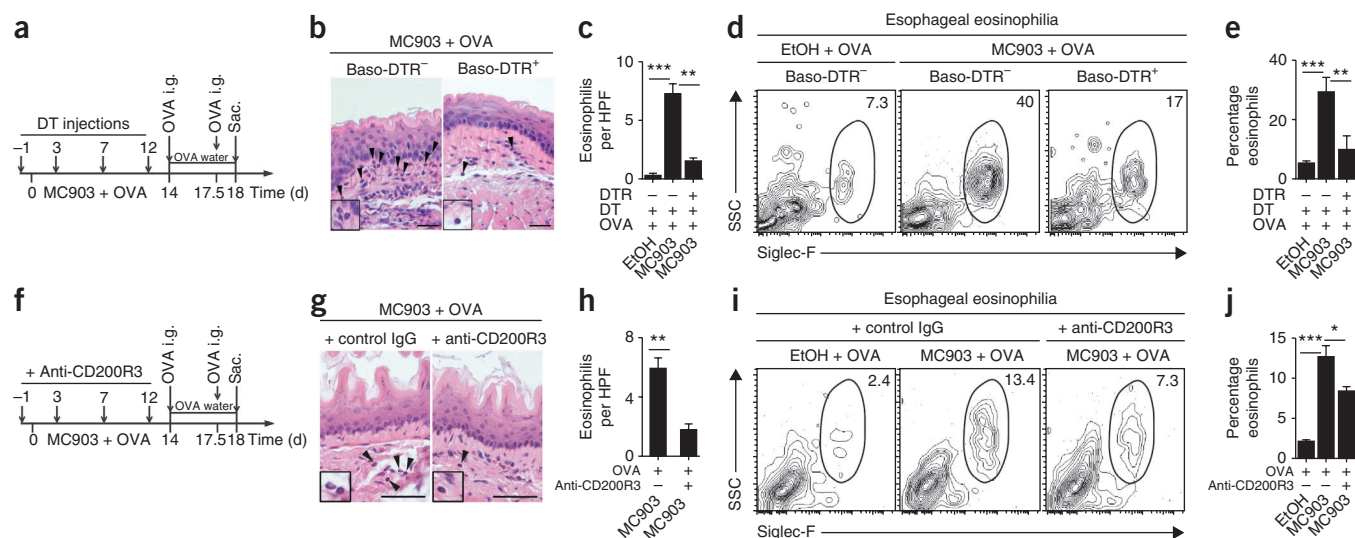


Figure 4 Basophils promote EoE-like disease. **(a)** Schematic of *in vivo* basophil depletion strategy. C57BL/6 (Baso-DTR⁻) or Baso-DTR⁺ mice were treated with diphtheria toxin (DT) during the course of epicutaneous sensitization. **(b)** Histological sections (H&E staining) from the esophagus. Arrowheads identify tissue-infiltrating eosinophils. Scale bar, 25 μ m. Insets: $\times 4$ magnification of whole image showing eosinophils. **(c)** Number of eosinophils per HPF in the esophagus. **(d)** Representative flow cytometry plots showing frequencies of eosinophils in esophageal tissues. Data in **b–d** are from one experiment (Baso-DTR⁻ EtOH + OVA, $n = 3$; Baso-DTR⁻ MC903 + OVA, $n = 3$; Baso-DTR⁺ MC903 + OVA, $n = 4$) and are representative of three independent replicates. **(e)** Frequencies of eosinophils in esophageal tissues, as measured by flow cytometry. Data depicted are from three pooled experiments (Baso-DTR⁻ EtOH + OVA, $n = 7$; Baso-DTR⁻ MC903 + OVA, $n = 10$; Baso-DTR⁺ MC903 + OVA, $n = 11$). **(f)** Schematic of *in vivo* basophil depletion strategy using CD200R3-specific mAb (anti-CD200R3) in WT BALB/c mice. **(g)** Histological sections (H&E staining) from the esophagus. Arrowheads identify tissue-infiltrating eosinophils. Scale bar, 50 μ m. Insets: $\times 4$ magnification of whole image showing eosinophils. **(h)** Number of eosinophils per HPF in the esophagus. **(i)** Representative flow cytometry plots showing frequencies of eosinophils in esophageal tissues. Data in **g–i** are from one experiment (EtOH + OVA + IgG, $n = 3$; MC903 + OVA + IgG, $n = 3$; MC903 + OVA + anti-CD200R3 mAb, $n = 4$) and are representative of three independent replicates. **(j)** Frequencies of eosinophils in esophageal tissues, as measured by flow cytometry. Data are from three pooled experiments (EtOH + OVA + IgG, $n = 8$; MC903 + OVA + IgG, $n = 9$; MC903 + OVA + anti-CD200R3 mAb, $n = 10$). All parameters were assessed 12 h after final oral antigen challenge. Data are from mice challenged twice with OVA. Results are shown as mean \pm s.e.m., and a nonparametric, two-tailed Mann-Whitney *t*-test or a nonparametric, one-way Kruskal-Wallis ANOVA with Dunn's *post hoc* testing were used to determine significance. * $P \leq 0.05$; ** $P \leq 0.01$; *** $P \leq 0.001$.

results indicate that basophils are major contributors to the pathogenesis of experimental EoE-like disease in mice and may represent a new therapeutic target to treat this disease in patients.

TSLP or basophils can be targeted to treat EoE-like disease

As TSLP and basophils were required during sensitization for the development of EoE-like disease in mice, we next tested whether the TSLP-basophil pathway could be therapeutically targeted to treat established EoE-like disease. First, we sensitized and challenged mice with OVA to establish EoE-like disease and then treated them systemically with either an isotype control or a neutralizing TSLP-specific mAb during repeated antigen challenge (Fig. 5a). Whereas mice with established EoE-like disease treated with a control antibody showed esophageal eosinophilia, mice that were treated with a TSLP-specific mAb had decreased esophageal eosinophilia, as measured histologically (Fig. 5b). Flow cytometric analysis also revealed that the total immune cell infiltrate and esophageal eosinophilia were significantly reduced in mice treated with a TSLP-specific mAb compared to mice treated with a control mAb (Fig. 5c,d).

To test whether basophils contributed to the maintenance of EoE-like disease, we treated mice with established EoE-like disease with an isotype control or basophil-depleting CD200R3-specific mAb during repeated OVA challenge (Fig. 5e). Similar to the results observed after neutralization of TSLP, specific depletion of basophils resulted in decreased esophageal eosinophilia, as measured histologically (Fig. 5f), and flow cytometric analysis showed a reduction in total immune cell infiltrate and eosinophil numbers in the esophagus (Fig. 5g,h). To test

whether neutralization of TSLP or depletion of basophils was also associated with a resolution of signs of esophageal dysfunction, we treated mice with established EoE-like disease with a control antibody, TSLP-specific mAb, or CD200R3-specific mAb and assessed them for the incidence of food impaction. Whereas we observed food impaction in about 30% of mice treated with a control antibody, we did not observe food impaction in mice in which TSLP or basophil responses were blocked (Fig. 5i). Taken together, these data demonstrate that TSLP neutralization or basophil depletion can be used to ameliorate inflammation and clinical symptoms of established experimental EoE-like disease in mice.

The TSLP-basophil axis is associated with EoE in humans

The roles of TSLP and basophils in experimental EoE-like disease in mice (Figs. 2 and 4) and the established association between a gain-of-function polymorphism in *TSLP* and EoE in human pediatric subjects^{10,11} prompted us to hypothesize that the TSLP-basophil pathway may contribute to the pathogenesis of EoE in humans. To assess whether the TSLP-basophil axis is active in human subjects with EoE, we examined TSLP expression and basophil responses in esophageal biopsies from a cohort of pediatric subjects. We stratified this patient population on the basis of the number of eosinophils counted in histologic sections from esophageal biopsies into the following groups: (i) control subjects without EoE, (ii) subjects with active EoE (≥ 15 eosinophils per HPF) and (iii) subjects with inactive EoE (< 15 eosinophils per HPF and a prior clinical history of active EoE) (Fig. 6a). In agreement with previous studies^{10,11},

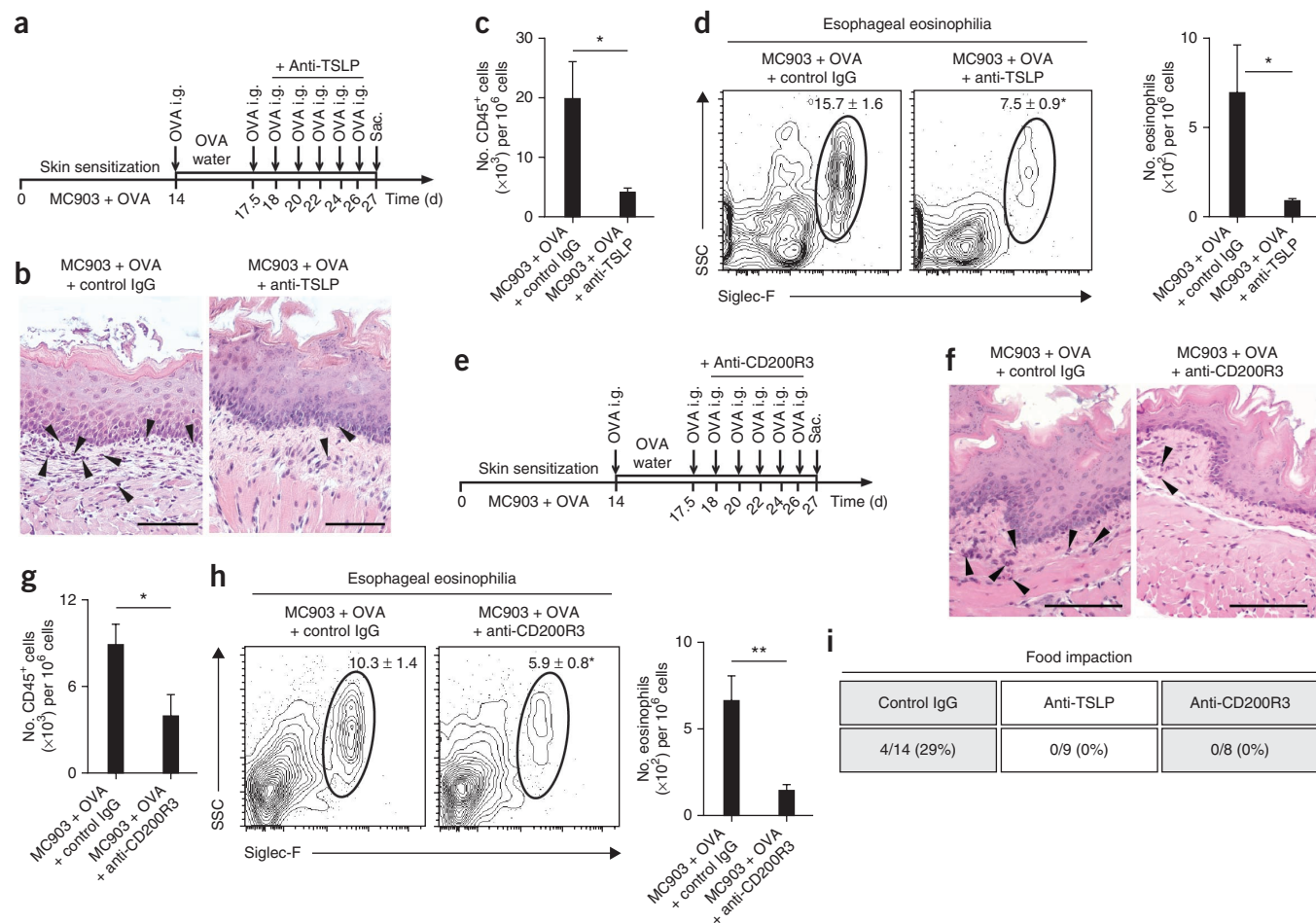


Figure 5 Neutralization of TSLP or depletion of basophils ameliorates established EoE-like disease. **(a)** Schematic of treatment with TSLP-specific mAb in WT BALB/c mice with established EoE-like disease. **(b)** Histological sections (H&E staining) from the esophagus. Arrowheads identify tissue-infiltrating eosinophils. Scale bar, 50 μ m. **(c)** Frequencies of CD45⁺ cells in esophageal tissues, as measured by flow cytometry. **(d)** Representative flow cytometry plots showing frequencies and total numbers of eosinophils in esophageal tissues. Data in **b–d** are from one experiment (MC903 + OVA + IgG, $n = 5$; MC903 + OVA + anti-TSLP mAb, $n = 5$) and are representative of three independent replicates. **(e)** Schematic of CD200R3-specific mAb basophil-depletion strategy in WT BALB/c mice in established EoE-like disease. **(f)** Histological sections (H&E staining) from the esophagus. Arrowheads identify tissue-infiltrating eosinophils. Scale bar, 50 μ m. **(g)** Frequencies of CD45⁺ cells in esophageal tissues, as measured by flow cytometry. **(h)** Representative flow cytometry plots showing frequencies and total numbers of eosinophils in esophageal tissues. Data in **f–h** are from one experiment (MC903 + OVA + IgG, $n = 4$; MC903 + OVA + anti-CD200R3 mAb, $n = 5$) and are representative of three independent replicates. **(i)** Quantified incidence of food impaction. All parameters were assessed 12 h after final oral antigen challenge. Data are from mice challenged repeatedly with OVA. Results are shown as mean \pm s.e.m., and a nonparametric, two-tailed Mann-Whitney t -test was used to determine significance. * $P \leq 0.05$; ** $P \leq 0.01$.

TSLP expression in esophageal biopsies was higher in subjects with active EoE compared to control subjects or subjects with inactive EoE (**Fig. 6b**). Immunohistochemical staining revealed that stratified squamous epithelial cells showed positive staining for TSLP in esophageal biopsies from subjects with active EoE (**Fig. 6c**). We then used flow cytometric analysis to identify and quantify the inflammatory cell infiltrate in biopsies. Notably, we observed higher frequencies of cells with a phenotype consistent with that of basophils (lin[−]CD49b⁺Fc ϵ RI⁺c-kit⁺2D7⁺) in esophageal biopsies from subjects with active EoE compared to those from control subjects or subjects with inactive EoE (**Fig. 6d,e**). Further, the frequency of basophils positively correlated (Spearman $r = 0.6638$) with the number of eosinophils counted per HPF in histological sections of esophageal biopsies (**Fig. 6f**). Additionally, we were able to stratify a cohort of adult subjects on the basis of the number of eosinophils counted in histologic sections (**Supplementary Fig. 7a**). Consistent with results observed in pediatric subjects (**Fig. 6d–f**), adult subjects with active

EoE had a higher (although not statistically significant) frequency of basophils in the esophageal biopsy, as measured using flow cytometry, that positively correlated (Spearman $r = 0.5282$) with the number of eosinophils counted per HPF in histological sections (**Supplementary Fig. 7b,c**). Collectively, these data indicate for the first time, to our knowledge, that the TSLP-basophil axis is associated with active EoE in pediatric and adult subjects.

These findings, coupled with the association between the development of EoE and a previously identified gain-of-function polymorphism in TSLP associated with TSLP overexpression (TSLP^{prisk})¹⁰, suggested that there may be an association between the TSLP^{prisk} polymorphism and enhanced basophil responses in human subjects with EoE. To directly test this, we assessed a separate cohort of pediatric subjects with active or inactive EoE genotyped for the presence of the TSLP^{prisk} polymorphism for basophil frequencies among peripheral blood mononuclear cells (PBMCs). Subjects who were homozygous or heterozygous for the TSLP^{prisk} polymorphism had significantly higher

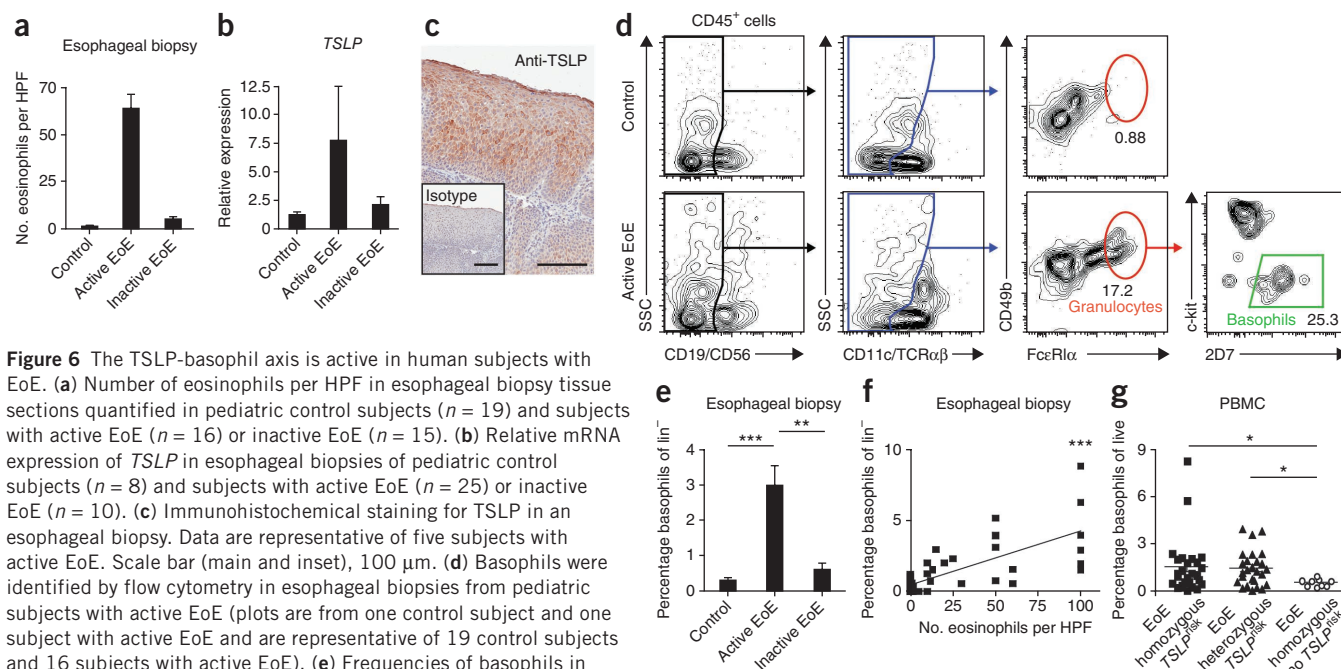


Figure 6 The TSLP-basophil axis is active in human subjects with EoE. **(a)** Number of eosinophils per HPF in esophageal biopsy tissue sections quantified in pediatric control subjects ($n = 19$) and subjects with active EoE ($n = 16$) or inactive EoE ($n = 15$). **(b)** Relative mRNA expression of *TSLP* in esophageal biopsies of pediatric control subjects ($n = 8$) and subjects with active EoE ($n = 25$) or inactive EoE ($n = 10$). **(c)** Immunohistochemical staining for TSLP in an esophageal biopsy. Data are representative of five subjects with active EoE. Scale bar (main and inset), 100 μ m. **(d)** Basophils were identified by flow cytometry in esophageal biopsies from pediatric subjects with active EoE (plots are from one control subject and one subject with active EoE and are representative of 19 control subjects and 16 subjects with active EoE). **(e)** Frequencies of basophils in the lin⁻ compartment (see Online Methods) in esophageal biopsies from pediatric control subjects ($n = 19$) and subjects with active EoE ($n = 16$) or inactive EoE ($n = 15$). **(f)** Correlation of frequencies of basophils in pediatric esophageal biopsies and the number of eosinophils per HPF observed histologically ($n = 50$) (Spearman $r = 0.6638$). **(g)** Frequencies of basophils in the PBMCs of pediatric subjects with EoE who were homozygous ($n = 26$) or heterozygous for the *TSLP*^{risk} polymorphism ($n = 26$) or who lacked the *TSLP*^{risk} polymorphism ($n = 9$), as identified by flow cytometry. All data are shown as mean \pm s.e.m., and a nonparametric, two-tailed Mann-Whitney *t*-test or a nonparametric, one-way Kruskal-Wallis ANOVA with Dunn's *post hoc* testing were used to determine significance. Correlation analysis was performed using a nonparametric Spearman correlation (sensitivity analyses were performed), and a linear regression of the data is shown. * $P \leq 0.05$; ** $P \leq 0.01$; *** $P \leq 0.001$.

basophil frequencies in their PBMCs than subjects with EoE who did not carry the *TSLP*^{risk} polymorphism (Fig. 6g), which suggests a genetic link between a gain-of-function *TSLP* polymorphism, increased peripheral basophil responses and EoE. As with most human inflammatory diseases such as asthma, inflammatory bowel disease and multiple sclerosis^{47–50}, the development of EoE probably involves a complex interplay of genetic and environmental factors. However, these data suggest a model in which patients that carry the *TSLP*^{risk} polymorphism have a predisposition toward *TSLP* overexpression and associated peripheral basophilia that may increase the likelihood of developing EoE after encounter with trigger antigens (Supplementary Fig. 8).

DISCUSSION

Here we describe a new mouse model in which epicutaneous sensitization to a model food antigen followed by oral antigen challenge results in EoE-like disease. We demonstrate that TSLP and basophils, but not IgE, are required for the development of experimental EoE-like disease in mice and that antibody-mediated neutralization of TSLP or depletion of basophils is effective in preventing the development of experimental EoE-like disease. Targeting TSLP or basophils was also effective in treating established EoE-like disease in mice. In addition, we identify for the first time the presence of enhanced basophil responses in the esophageal biopsy tissue of human subjects with EoE and a genetic link between a gain-of-function polymorphism in *TSLP* and increased peripheral basophil responses.

Although all experimental model systems have limitations and do not recapitulate the diversity of symptoms reported in humans, the model of EoE-like disease we report here is associated with several

characteristics of EoE in humans, including esophageal eosinophilia and associated esophageal dysfunction. In addition, this model is also characterized by gastrointestinal eosinophilia and systemic T_H2 cytokine responses. EoE in humans is defined as a disease associated with eosinophilia in the esophagus. However, patients with EoE often suffer from coexisting allergic disorders such as atopic dermatitis, allergic rhinitis, asthma or intestinal food allergy^{2,7,51}. These observations suggest that a subset of individuals with EoE with coexisting allergic diseases may present with manifestations of allergic disease at tissue sites outside of the esophagus⁵². Thus, the mouse model of EoE-like disease we describe may recapitulate a pan-allergic disease state present in some humans who have EoE and suffer from additional allergic diseases. Although EoE-like disease in this model develops independently of IgE and is dependent on TSLP and basophils, further studies will be required to investigate whether the gastrointestinal eosinophilia in this model is dependent on IgE or TSLP-elicited basophils.

Previous studies in mouse models and humans have identified various immunological factors that are associated with EoE^{1–3,31–34,53–58}. However, recent clinical trials that have targeted some of these factors, including IgE and IL-5, have failed to ameliorate symptoms of disease^{2,41,42,44,59,60}, suggesting that these factors may not be essential for the pathogenesis of EoE. The demonstration that EoE-like disease in mice can develop independently of IgE but is dependent on TSLP and basophils may explain why previous clinical trials employing other candidate biologic therapies have not been successful. The identification of a role for TSLP and basophils in experimental EoE-like disease in mice, coupled with the association between TSLP and basophil responses and EoE in humans, indicate

that targeting the TSLP-basophil axis may offer new opportunities for the clinical management of EoE in patients.

METHODS

Methods and any associated references are available in the [online version of the paper](#).

Note: Supplementary information is available in the online version of the paper.

ACKNOWLEDGMENTS

We thank members of the Artis laboratory for discussions and critical reading of the manuscript. Research in the Artis lab is supported by the US National Institutes of Health (AI061570, AI087990, AI074878, AI095776, AI102942, AI095466, AI09560 and AI097333 to D.A.), the Swiss National Science Foundation Prospective and Advanced Research Fellowships (PBBEP3_130438 and PA00P3_136468 to M.N.), the US National Institutes of Health (T32-AI060516 and F32-AI098365 to E.D.T.W., T32-AR007465 and KL2-RR024132 to B.S.K., F32-AI085828 to M.C.S., AI091759 to M.G.N. and K08-AI089982 to A.C.), the Australian National Health and Medical Research Council Overseas Biomedical Fellowship (613718 to P.R.G.), the State of Pennsylvania (SAP 4100042728 to P.M.S. and H.H.), the Burroughs Wellcome Fund Investigator in Pathogenesis of Infectious Disease Award (D.A.) and the Crohn's and Colitis Foundation of America (D.A.). This work was supported by the US National Institutes of Health/US National Institute of Diabetes and Digestive and Kidney Diseases P30 Center for Molecular Studies in Digestive and Liver Diseases (P30-DK050306), its pilot grant program and scientific core facilities (Molecular Pathology and Imaging, Molecular Biology, Cell Culture and Mouse) and the Joint Penn-Children's Hospital of Philadelphia Center in Digestive, Liver and Pancreatic Medicine and its pilot grant program. We also thank the Matthew J. Ryan Veterinary Hospital Pathology Lab and the Abramson Cancer Center Flow Cytometry and Cell Sorting Resource Laboratory (partially supported by US National Cancer Institute Comprehensive Cancer Center Support Grant (P30-CA016520)), the Skin Disease Research Center (supported by P30-AR057217) and the Electron Microscopy Resource Laboratory for technical advice and support. J.M.S. and K.R.R. acknowledge support from The Children's Hospital of Philadelphia Institutional Development Fund, and J.M.S. also acknowledges support from the US Department of Defense (A-16809.2). Human tissue samples were obtained by M.-L.W. and A.J.B., funded by Abbot Nutrition (ANUS1013). Research in the Zhou lab is supported by the US National Institutes of Health (R01EB010071) and the Lehigh University start-up fund. The studies described here were supported in part by the Institute for Translational Medicine and Therapeutics Transdisciplinary Program in Translational Medicine and Therapeutics (UL1-RR024134 from the US National Center for Research Resources). The authors also wish to thank P. Just and N. Ruiz at eBioscience for samples of flow cytometry reagents for human basophil panel development, support and invaluable technical advice. CD200R3-specific mAb (clone Ba103) was provided by H. Karasuyama (Tokyo Medical and Dental University Graduate School). The content is solely the responsibility of the authors and does not represent the official views of the US National Center for Research Resources or the US National Institutes of Health.

AUTHOR CONTRIBUTIONS

M.N., E.D.T.W., B.S.K., M.C.S., P.R.G., M.G.N., A.B.M., A.A., C.Z. and D.A. designed and performed experiments. A.J.B., K.R.R., P.M.-K., A.C., G.W.F., M.-L.W. and J.M.S. obtained human pediatric and adult esophageal biopsies and peripheral blood samples. K.R.C. analyzed pediatric esophageal biopsy histology, and D.A.H. and T.B.-W. coordinated patient care and clinical studies. A.E.M. and Q.J.S. provided CPE, M.K. provided Baso-DTR mice, K.O.-N. and H.K. provided CD200R3-specific mAb, M.R.C. provided TSLPR-deficient mice and TSLP reagents, J.H.Y. and R.d.W.M. performed staining for human TSLP, and P.M.S. and H.H. provided genotype information on pediatric patients with EoE. M.N., E.D.T.W., B.S.K., M.C.S., P.R.G., A.A., C.Z., M.-L.W., J.M.S. and D.A. analyzed the data. M.N., E.D.T.W., M.C.S. and D.A. wrote the manuscript, and all authors critically reviewed the manuscript.

COMPETING FINANCIAL INTERESTS

The authors declare competing financial interests: details are available in the [online version of the paper](#).

Reprints and permissions information is available online at <http://www.nature.com/reprints/index.html>.

1. Spergel, J.M. Eosinophilic esophagitis in adults and children: evidence for a food allergy component in many patients. *Curr. Opin. Allergy Clin. Immunol.* **7**, 274–278 (2007).
2. Liacouras, C.A. *et al.* Eosinophilic esophagitis: updated consensus recommendations for children and adults. *J. Allergy Clin. Immunol.* **128**, 3–20.e26 (2011).
3. Abonia, J.P. & Rothenberg, M.E. Eosinophilic esophagitis: rapidly advancing insights. *Annu. Rev. Med.* **63**, 421–434 (2012).
4. Straumann, A. & Simon, H.U. Eosinophilic esophagitis: escalating epidemiology? *J. Allergy Clin. Immunol.* **115**, 418–419 (2005).
5. Kapel, R.C. *et al.* Eosinophilic esophagitis: a prevalent disease in the United States that affects all age groups. *Gastroenterology* **134**, 1316–1321 (2008).
6. Straumann, A. & Schoepfer, A.M. Therapeutic concepts in adult and paediatric eosinophilic esophagitis. *Nat. Rev. Gastroenterol. Hepatol.* **9**, 697–704 (2012).
7. Arora, A.A., Weiler, C.R. & Katzka, D.A. Eosinophilic esophagitis: allergic contribution, testing, and management. *Curr. Gastroenterol. Rep.* **14**, 206–215 (2012).
8. Markowitz, J.E., Spergel, J.M., Ruchelli, E. & Liacouras, C.A. Elemental diet is an effective treatment for eosinophilic esophagitis in children and adolescents. *Am. J. Gastroenterol.* **98**, 777–782 (2003).
9. Mulder, D.J. & Justinich, C.J. B cells, IgE and mechanisms of type I hypersensitivity in eosinophilic oesophagitis. *Gut* **59**, 6–7 (2010).
10. Rothenberg, M.E. *et al.* Common variants at 5q22 associate with pediatric eosinophilic esophagitis. *Nat. Genet.* **42**, 289–291 (2010).
11. Sherrill, J.D. *et al.* Variants of thymic stromal lymphopoietin and its receptor associate with eosinophilic esophagitis. *J. Allergy Clin. Immunol.* **126**, 160–165.e163 (2010).
12. Ziegler, S.F. The role of thymic stromal lymphopoietin (TSLP) in allergic disorders. *Curr. Opin. Immunol.* **22**, 795–799 (2010).
13. Ramasamy, A. *et al.* A genome-wide meta-analysis of genetic variants associated with allergic rhinitis and grass sensitization and their interaction with birth order. *J. Allergy Clin. Immunol.* **128**, 996–1005 (2011).
14. Liu, M. *et al.* Genetic variants of TSLP and asthma in an admixed urban population. *PLoS ONE* **6**, e25099 (2011).
15. Hirota, T. *et al.* Genome-wide association study identifies three new susceptibility loci for adult asthma in the Japanese population. *Nat. Genet.* **43**, 893–896 (2011).
16. Hunninghake, G.M. *et al.* TSLP polymorphisms are associated with asthma in a sex-specific fashion. *Allergy* **65**, 1566–1575 (2010).
17. Siracusa, M.C. *et al.* TSLP promotes interleukin-3-independent basophil haematopoiesis and type 2 inflammation. *Nature* **477**, 229–233 (2011).
18. Siracusa, M.C., Wojno, E.D. & Artis, D. Functional heterogeneity in the basophil cell lineage. *Adv. Immunol.* **115**, 141–159 (2012).
19. Giacomini, P.R. *et al.* Thymic stromal lymphopoietin-dependent basophils promote TH2 cytokine responses following intestinal helminth infection. *J. Immunol.* **189**, 4371–4378 (2012).
20. Liu, Y.J. *et al.* TSLP: an epithelial cell cytokine that regulates T cell differentiation by conditioning dendritic cell maturation. *Annu. Rev. Immunol.* **25**, 193–219 (2007).
21. Soumelis, V. *et al.* Human epithelial cells trigger dendritic cell mediated allergic inflammation by producing TSLP. *Nat. Immunol.* **3**, 673–680 (2002).
22. Hsieh, K.Y., Tsai, C.C., Wu, C.H. & Lin, R.H. Epicutaneous exposure to protein antigen and food allergy. *Clin. Exp. Allergy* **33**, 1067–1075 (2003).
23. Lack, G. Update on risk factors for food allergy. *J. Allergy Clin. Immunol.* **129**, 1187–1197 (2012).
24. van den Oord, R.A. & Sheikh, A. Filaggrin gene defects and risk of developing allergic sensitization and allergic disorders: systematic review and meta-analysis. *Br. Med. J.* **339**, b2433 (2009).
25. Li, M. *et al.* Topical vitamin D3 and low-calcemic analogs induce thymic stromal lymphopoietin in mouse keratinocytes and trigger an atopic dermatitis. *Proc. Natl. Acad. Sci. USA* **103**, 11736–11741 (2006).
26. Li, M. *et al.* Induction of thymic stromal lymphopoietin expression in keratinocytes is necessary for generating an atopic dermatitis upon application of the active vitamin D3 analogue MC903 on mouse skin. *J. Invest. Dermatol.* **129**, 498–502 (2009).
27. Leyva-Castillo, J.M., Hener, P., Jiang, H. & Li, M. TSLP produced by keratinocytes promotes allergen sensitization through skin and thereby triggers atopic march in mice. *J. Invest. Dermatol.* **133**, 154–163 (2013).
28. DeBrosse, S.D. *et al.* Long-term outcomes in pediatric-onset esophageal eosinophilia. *J. Allergy Clin. Immunol.* **128**, 132–138 (2011).
29. Huang, D. *et al.* Optical coherence tomography. *Science* **254**, 1178–1181 (1991).
30. Zhou, C. *et al.* Characterization of buried glands before and after radiofrequency ablation by using 3-dimensional optical coherence tomography (with videos). *Gastrointest. Endosc.* **76**, 32–40 (2012).
31. Bhattacharya, B. *et al.* Increased expression of eotaxin-3 distinguishes between eosinophilic esophagitis and gastroesophageal reflux disease. *Hum. Pathol.* **38**, 1744–1753 (2007).
32. Blanchard, C. *et al.* A striking local esophageal cytokine expression profile in eosinophilic esophagitis. *J. Allergy Clin. Immunol.* **127**, 208–217, 217.e1–7 (2011).
33. Hsu Blatman, K.S., Gonsalves, N., Hirano, I. & Bryce, P.J. Expression of mast cell-associated genes is upregulated in adult eosinophilic esophagitis and responds to steroid or dietary therapy. *J. Allergy Clin. Immunol.* **127**, 1307–1308.e3 (2011).

34. Justinich, C.J. *et al.* Activated eosinophils in esophagitis in children: a transmission electron microscopic study. *J. Pediatr. Gastroenterol. Nutr.* **25**, 194–198 (1997).
35. Oyoshi, M.K., Larson, R.P., Ziegler, S.F. & Geha, R.S. Mechanical injury polarizes skin dendritic cells to elicit a T_H2 response by inducing cutaneous thymic stromal lymphopoietin expression. *J. Allergy Clin. Immunol.* **126**, 976–984, 984.e1–5 (2010).
36. Yoo, J. *et al.* Spontaneous atopic dermatitis in mice expressing an inducible thymic stromal lymphopoietin transgene specifically in the skin. *J. Exp. Med.* **202**, 541–549 (2005).
37. Jessup, H.K. *et al.* Intradermal administration of thymic stromal lymphopoietin induces a T cell- and eosinophil-dependent systemic T_H2 inflammatory response. *J. Immunol.* **181**, 4311–4319 (2008).
38. Finkelman, F.D. Anaphylaxis: lessons from mouse models. *J. Allergy Clin. Immunol.* **120**, 506–515 (2007).
39. Lucendo, A.J. *et al.* Immunophenotypic characterization and quantification of the epithelial inflammatory infiltrate in eosinophilic esophagitis through stereology: an analysis of the cellular mechanisms of the disease and the immunologic capacity of the esophagus. *Am. J. Surg. Pathol.* **31**, 598–606 (2007).
40. Vicario, M. *et al.* Local B cells and IgE production in the oesophageal mucosa in eosinophilic oesophagitis. *Gut* **59**, 12–20 (2010).
41. Rocha, R. *et al.* Omalizumab in the treatment of eosinophilic esophagitis and food allergy. *Eur. J. Pediatr.* **170**, 1471–1474 (2011).
42. Froughi, S. *et al.* Anti-IgE treatment of eosinophil-associated gastrointestinal disorders. *J. Allergy Clin. Immunol.* **120**, 594–601 (2007).
43. Stone, K.D. & Prussin, C. Immunomodulatory therapy of eosinophil-associated gastrointestinal diseases. *Clin. Exp. Immunol.* **38**, 1858–1865 (2008).
44. Sampson, H.A. *et al.* A phase II, randomized, double-blind, parallel-group, placebo-controlled oral food challenge trial of Xolair (omalizumab) in peanut allergy. *J. Allergy Clin. Immunol.* **127**, 1309–1310.e1 (2011).
45. Sawaguchi, M. *et al.* Role of mast cells and basophils in IgE responses and in allergic airway hyperresponsiveness. *J. Immunol.* **188**, 1809–1818 (2012).
46. Obata, K. *et al.* Basophils are essential initiators of a novel type of chronic allergic inflammation. *Blood* **110**, 913–920 (2007).
47. Mukherjee, A.B. & Zhang, Z. Allergic asthma: influence of genetic and environmental factors. *J. Biol. Chem.* **286**, 32883–32889 (2011).
48. Sun, L., Nava, G.M. & Stappenbeck, T.S. Host genetic susceptibility, dysbiosis, and viral triggers in inflammatory bowel disease. *Curr. Opin. Gastroenterol.* **27**, 321–327 (2011).
49. Renz, H. *et al.* Gene-environment interactions in chronic inflammatory disease. *Nat. Immunol.* **12**, 273–277 (2011).
50. Gourraud, P.A., Harbo, H.F., Hauser, S.L. & Baranzini, S.E. The genetics of multiple sclerosis: an up-to-date review. *Immunol. Rev.* **248**, 87–103 (2012).
51. Brown-Whitehorn, T.F. & Spergel, J.M. The link between allergies and eosinophilic esophagitis: implications for management strategies. *Expert Rev. Clin. Immunol.* **6**, 101–109 (2010).
52. Straumann, A. *et al.* Cytokine expression in healthy and inflamed mucosa: probing the role of eosinophils in the digestive tract. *Inflamm. Bowel Dis.* **11**, 720–726 (2005).
53. Akei, H.S., Mishra, A., Blanchard, C. & Rothenberg, M.E. Epicutaneous antigen exposure primes for experimental eosinophilic esophagitis in mice. *Gastroenterology* **129**, 985–994 (2005).
54. Mavi, P., Rajavelu, P., Rayapudi, M., Paul, R.J. & Mishra, A. Esophageal functional impairments in experimental eosinophilic esophagitis. *Am. J. Physiol. Gastrointest. Liver Physiol.* **302**, G1347–G1355 (2012).
55. Rajavelu, P., Rayapudi, M., Moffitt, M. & Mishra, A. Significance of para-esophageal lymph nodes in food or aeroallergen-induced iNKT cell-mediated experimental eosinophilic esophagitis. *Am. J. Physiol. Gastrointest. Liver Physiol.* **302**, G645–G654 (2012).
56. Mishra, A., Schlotman, J., Wang, M. & Rothenberg, M.E. Critical role for adaptive T cell immunity in experimental eosinophilic esophagitis in mice. *J. Leukoc. Biol.* **81**, 916–924 (2007).
57. Mishra, A. & Rothenberg, M.E. Intratracheal IL-13 induces eosinophilic esophagitis by an IL-5, eotaxin-1, and STAT6-dependent mechanism. *Gastroenterology* **125**, 1419–1427 (2003).
58. Mishra, A., Hogan, S.P., Brandt, E.B. & Rothenberg, M.E. IL-5 promotes eosinophil trafficking to the esophagus. *J. Immunol.* **168**, 2464–2469 (2002).
59. Spergel, J.M. *et al.* Reslizumab in children and adolescents with eosinophilic esophagitis: results of a double-blind, randomized, placebo-controlled trial. *J. Allergy Clin. Immunol.* **129**, 456–463, 463.e1–3 (2012).
60. Castro, M. *et al.* Reslizumab for poorly controlled, eosinophilic asthma: a randomized, placebo-controlled study. *Am. J. Respir. Crit. Care Med.* **184**, 1125–1132 (2011).

ONLINE METHODS

Mice. Male and female BALB/c and C57BL/6 mice were purchased from the Jackson Laboratories. BALB/c *Tslpr*^{+/+} and BALB/c *Tslpr*^{-/-} mice were provided by Amgen, through Charles River Laboratories. BALB/c *Igh*-7^{-/-} mice and C57BL/6 Baso-DTR mice were bred at the University of Pennsylvania. All mice were used at 8–12 weeks of age, and all experiments employed age-, gender- and genetic strain-matched controls to account for any variations in data sets compared across experiments. Mice were bred and housed in specific pathogen-free conditions at the University of Pennsylvania. Mice requiring medical attention were provided with appropriate veterinary care by a licensed veterinarian and were excluded from the experiments described. No other exclusion criteria existed. All experiments were performed under the University of Pennsylvania Institutional Animal Care and Use Committee (IACUC) approved protocols and in accordance with its guidelines.

Reagents and treatments. Mice were treated daily with 2 nmol MC903 (calcipotriol, Tocris Bioscience) in 20 μ l of 100% EtOH applied to the ears in the presence of 100 μ g OVA for 14 d. As a vehicle control, the same volume of EtOH and OVA was applied. For tape-stripping, mice were shaved on the back, tape-stripped six times with scotch sealing tape and sensitized with 100 μ g OVA or saline as control daily for 14 d. For TSLP injections, mice were subcutaneously injected with 5 μ g rTSLP in the presence of 100 μ g OVA on days 0, 3, 6, 9 and 12. For controls, mice were injected subcutaneously with PBS or rTSLP alone. For CPE sensitization, CPE was made from whole roasted peanuts (Sainsbury's Ltd.) sterilized by gamma irradiation (Lillico Biotech) that were ground in an airflow cabinet using a mortar and pestle. The resulting paste was solubilized in pH 7.4 PBS (Gibco) and sonicated for two 20-min periods, with mixing in between. The solution was then filtered through a 75- μ m tissue filter (BD Biosciences) to remove large particles of debris. Lipopolysaccharide content was tested (Lonza) and reported less than 0.006 ng mL⁻¹. Mice were treated daily with 2 nmol MC903 in 20 μ l of 100% EtOH on ears in the presence of 100 μ g CPE for 14 d. As a vehicle control, the same volume of EtOH and CPE was applied. Mice were challenged i.g. with 50 mg OVA or 10 mg CPE on days 14 and 17.5 and killed on day 18. Upon first i.g. OVA or CPE challenge, mice were continuously fed water containing 1.5 g L⁻¹ OVA or given continuous access to whole roasted peanut. Mice subjected to repeated challenge with OVA to induce prolonged inflammation in the esophagus were challenged i.g. with 50 mg OVA on days 14, 17.5, 18, 20, 22, 24 and 26 and killed on day 27. For depletion with TSLP-specific mAb¹⁷, mice were injected with 500 μ g of control IgG or TSLP-specific mAb commercially produced by Amgen intraperitoneally every 3 d during the course of the experiment starting at day -1 or every other day starting at day 18. For basophil depletion by diphtheria toxin treatment, Baso-DTR⁺ or Baso-DTR⁻ littermate control mice were treated with 500 ng diphtheria toxin (Sigma) intraperitoneally on days -1, 3, 7 and 12. For depletion with CD200R3-specific mAb (Ba103)⁴⁶, mice were injected with 100 μ g of control IgG or CD200R3-specific mAb (clone Ba103, provided by H. Karasuyama) intravenously every 4 d during the course of the experiment starting at day -1 or every other day starting at day 18. To assess food impaction in the esophagus, mice exposed to prolonged esophageal inflammation were fasted for at least 30 min and up to 2 h. Mice were then killed, and their esophagi were examined for the presence of impacted food.

Cohort of human subjects with eosinophilic esophagitis. Pediatric participants from a cohort of control subjects or subjects with EoE at the University of Pennsylvania Penn-Children's Hospital of Philadelphia (CHOP) Joint Center for Digestive, Liver and Pancreatic Medicine or the Center for Pediatric Eosinophilic Disorders at CHOP were analyzed and were provided under a CHOP IRB to M.-L.W. and A.J.B. Adult participants from a cohort of control subjects or subjects with EoE being treated at the Hospital of the University of Pennsylvania Division of Gastroenterology were also assessed and were provided under a University of Pennsylvania IRB to G.W.F. and P.M.-K. Written consent was obtained from all participants or their parents or legal guardians, and for pediatric participants, verbal assent from the child was additionally obtained. Subjects defined as having EoE had no other chronic condition except asthma, allergic rhinitis, food allergy, urticaria or atopic dermatitis. Control subjects presented with epigastric abdominal pain but had normal endoscopic and microscopic results. Pediatric subjects with EoE were on proton pump

inhibitor therapy, but subjects on systemic corticosteroid treatment or antibiotics were excluded. Subjects with active EoE had an esophageal eosinophil count of ≥ 15 per HPF after 8 weeks of treatment with a proton pump inhibitor. Subjects with inactive EoE had previously been diagnosed with active EoE but had an esophageal eosinophil count of < 15 per HPF at the time of sample collection. During routine endoscopy, three esophageal biopsies were collected for histological analysis of esophageal eosinophil counts. During the same procedure, two esophageal tissue biopsies were collected for research purposes, for either real-time PCR, immunohistochemistry or flow cytometry. For flow cytometry, single-cell suspensions were made by filtering the mechanically disrupted tissue through a 70- μ m filter (BD Biosciences) for flow cytometry. Peripheral blood from pediatric subjects from a cohort of control subjects or subjects with active or inactive EoE that were genotyped for a gain-of-function *TSLP* polymorphism at the University of Pennsylvania Penn-CHOP Joint Center for Digestive, Liver and Pancreatic Medicine or the Center for Pediatric Eosinophilic Disorders at CHOP was analyzed and was provided under a CHOP IRB to J.M.S. and K.R.R. Written consent was obtained from all participants or their parents or legal guardians, and for pediatric participants, verbal assent from the child was additionally obtained. Peripheral blood was collected by venipuncture, and serum was isolated. PBMCs were isolated by Ficoll gradient as previously described¹⁷, and cells were analyzed by flow cytometry. For genotyping of pediatric subjects with EoE, all samples were genotyped on either the Illumina HumanHap 550 or 610 BeadChips according to the manufacturer's protocols. Data normalization and canonical genotype clustering were carried out using the Illumina Genome Studio package. Samples with call rate $< 98\%$ were excluded from further analysis.

Human real-time PCR and immunohistochemistry. For real-time PCR analysis of gene expression in human esophageal biopsies, human subject biopsy samples were collected and placed in RNA^{later} (Ambion). RNA was isolated using the mirVana miRNA Isolation Kit according to the manufacturer's recommendations (Ambion) and reverse transcribed using a high-capacity cDNA reverse transcriptase kit (Applied Biosystems). Quantitative real-time PCR was performed using the Taqman Fast Universal PCR Master Mix kit and preformulated TaqMan Gene Expression Assays for *TSLP* (Applied Biosystems). Reactions were performed in triplicate using 96-well optical plates on a StepOnePlus Real-Time PCR System (Applied Biosystems). GAPDH was used as an endogenous control to normalize the samples using the C_T method of relative quantification, where C_T is the threshold cycle. For immunohistochemical staining for human TSLP, human esophageal biopsies were embedded in paraffin and sectioned. Sections were deparaffinized and stained with a primary human TSLP-specific mAb or an isotype control antibody (validated by J.H. Yearley and R. de Waal Malefyt and commercially produced by Merck Research Laboratories), and positive staining was visualized using the DAB substrate kit (Vector Laboratories).

Flow cytometry. For mouse studies, esophageal tissues of two or three mice were pooled within each replicate experiment, opened longitudinally, digested in 1 mg mL⁻¹ collagenase/DNase (Roche) for 30 min, and mashed through 70- μ m nylon mesh filters. Single-cell suspensions were incubated with Aqua Live/Dead Fixable Dye (Invitrogen) for dead cell exclusion and stained with fluorochrome-conjugated mAbs purchased from eBioscience specific for mouse CD3 ϵ (145-2C11, 1:300), CD4 (GK1.5, 1:300), CD8 (53-6.7, 1:300), NK1.1 (PK136, 1:300), CD19 (eBio1D3, 1:300), Fc ϵ R1 (MAR-1, 1:200), IgE (23G3, 1:200), CD45 (30-F11, 1:200), CD49b (DX5, 1:200), CD117 (c-kit, 1:200), fluorochrome-conjugated mAbs purchased from Biolegend specific for mouse CD11c (N418, 1:200), CD5 (53-7.3, 1:300), B220 (RA3-6B2, 1:300) and a fluorochrome-conjugated mAb purchased from BD Bioscience specific for mouse Siglec-F (E50-2440, 1:200), or fluorochrome-conjugated mAbs purchased from eBioscience specific for human CD19 (HIB19, 1:200), CD45 (HI30, 1:100), CD49b (eBioY418, 1:200), Fc ϵ R1 (AER-37, 1:50), CD123 (6H6, 1:100) and c-kit (104D2, 1:30) or fluorochrome-conjugated mAbs purchased from BD Biosciences specific for human CD56 (B159, 1:200), CD11c (B-ly6, 1:200) and TCR $\alpha\beta$ (IP26, 1:200). For intracellular staining, surface-stained cells were washed, fixed in 2% paraformaldehyde, permeabilized using eBioscience Permeabilization Buffer (eBioscience) according to manufacturer instructions, stained intracellularly with human 2D7-specific mAb (2D7, 1:25) (eBioscience), washed and

resuspended in flow cytometry buffer. All cells were run on a four-laser 14-color LSR II (BD Biosciences), and FlowJo 8.7.1 (Tree Star) was used to analyze data. Mouse eosinophils were identified as live, lin^- (CD3,CD5,CD19,CD11c,NK1.1), CD45⁺Siglec-F⁺ side-scatter (SSC)-high cells. Mouse basophils were identified as live, lin^- (CD3,CD5,CD19,CD11c,NK1.1), c-kit⁺CD49b⁺IgE⁺ cells (or as FcεRI⁺ cells in *Igh-7^{-/-}* mice). Human basophils in the esophageal biopsy were identified as live, lin^- (CD19,CD56,CD11c,TCRαβ), CD49b⁺FcεRI⁺c-kit⁺2D7⁺ cells. Human basophils in the PBMCs were identified as live, lin^- (CD19,CD56,CD11c,TCRαβ), CD123⁺FcεRI⁺ cells.

Optical coherence tomography. An OCT system operating at 1.3-μm center wavelength at 47 kHz axial scan rate (~30 frames per s) was developed and used for obtaining volumetric images of freshly excised mouse esophagus. The axial and transverse resolutions were 6 μm and 10 μm in tissue, respectively, and the imaging depth was approximately 2 mm, sufficient to image through the entire thickness of the mouse esophagus. Prior to OCT imaging, the esophagus was removed from the mouse, and a plastic tube with 0.75-mm outer diameter was inserted, allowing for the luminal surface to be clearly differentiated in cross-sectional images. The esophagus was immersed in saline solution to remove light reflection from the surface. Subsequently, three-dimensional OCT images were obtained from multiple locations along the esophagus, with each data set covering $3 \times 1.5 \times 1.5 \text{ mm}^3$. The thickness values of the squamous epithelial layer were measured from cross-sectional OCT images every 200 μm along the esophagus within each data set. Average squamous epithelial thickness values from the middle of the esophagus were calculated from each mouse by an investigator blinded to group allocations and were used for comparison between different groups.

Mouse cell cultures, ELISA, real-time PCR, histology and electron microscopy. To measure spontaneous release of TSLP, whole ears were incubated for 12 h in complete culture medium (DMEM, 10% FBS), and cell-free supernatants were stored for a TSLP ELISA using a commercially available kit (eBioscience). For antigen re-stimulation, splenocytes or mesenteric lymph node cells were isolated, and single-cell suspensions were stimulated with 200 μg OVA for 72 h. Cell-free supernatants were used for standard sandwich ELISA. Antigen-specific IgE responses were measured as described previously⁶¹. For histological analysis, at necropsy, the esophagus was fixed in 4% paraformaldehyde and embedded in paraffin, and 5-μm sections were cut and stained with hematoxylin and eosin (H&E). For immunofluorescence, sections were deparaffinized and stained with biotinylated Siglec-F-specific mAb from R&D Systems (BAF1706, 1:200), followed by secondary staining with Cy3-conjugated streptavidin (Jackson Laboratory) and counterstaining with DAPI (Molecular Probes). For EM, esophageal tissues were fixed with 2.5% glutaraldehyde, 2.0% paraformaldehyde in 0.1 M sodium cacodylate buffer, pH 7.4, overnight at 4 °C. After buffer washes, the samples were post-fixed in 2.0% osmium tetroxide for

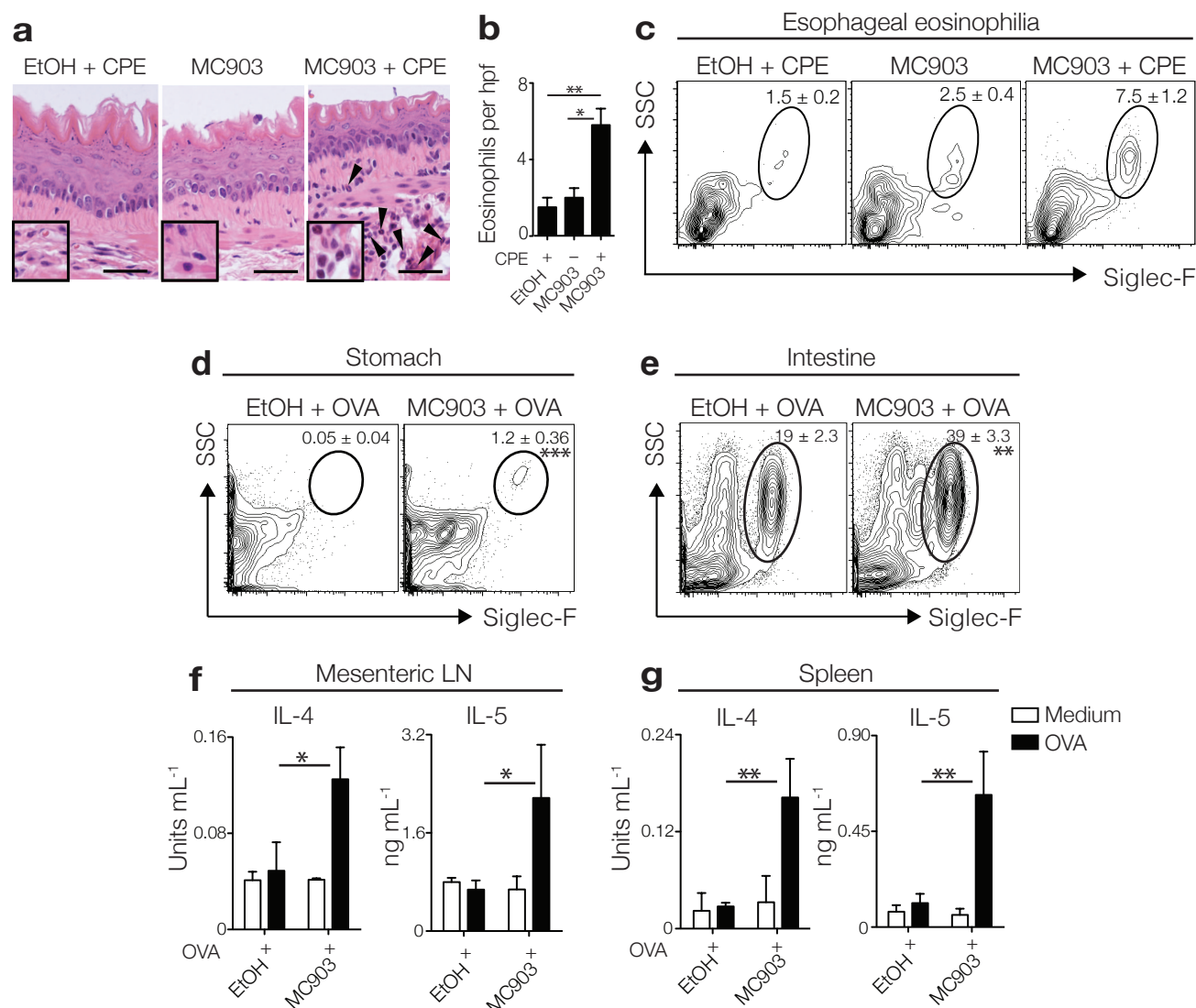
1 h at room temperature and rinsed in dH₂O before *en bloc* staining with 2% uranyl acetate. After dehydration through a graded ethanol series, the tissue was infiltrated and embedded in Embed-812 (Electron Microscopy Sciences). Thin sections were stained with uranyl acetate and lead citrate and examined with a JEOL 1010 electron microscope fitted with a Hamamatsu digital camera and AMT Advantage image capture software. For real-time PCR analysis, RNA was isolated from esophageal tissue using an RNeasy mini kit (Qiagen) or the mirVana miRNA isolation kit (Ambion) according to the manufacturer's instructions. cDNA was generated using a SuperscriptII reverse transcription kit (Invitrogen). Real-time quantitative PCR was performed on cDNA using SYBR green master mix (Applied Biosystems) and commercially available primer sets from Qiagen (Quantitect primer assays). Samples were run on a real-time PCR system (ABI 7500; Applied Biosystems), normalized to β-actin and displayed as fold induction over controls.

Statistical analysis. Results are shown as mean ± s.e.m. To determine group sizes necessary for adequate statistical power, power analysis was performed using preliminary data sets for all analyses presented. Mice were assigned at random to treatment groups for all mouse studies. Mouse studies were not performed in a blinded fashion, except where indicated. Analyses of basophil responses in esophageal biopsy samples and peripheral blood were conducted in such a manner that the investigator was blinded to the disease state (number of eosinophils per HPF in the biopsy) and *TSLP* genotype until after flow cytometric analyses were completed. Analysis of *TSLP* expression levels in the biopsies of control subjects and those with EoE were not performed in a blinded fashion. All inclusion and exclusion criteria for mouse and human studies were pre-established. For mouse studies, statistical significance was determined using a nonparametric, two-tailed Mann-Whitney *t*-test, a nonparametric, one-way Kruskal-Wallis ANOVA test followed by Dunn's *post hoc* testing or a nonparametric, two-way ANOVA followed by Bonferroni's *post hoc* testing. For human studies, a nonparametric, two-tailed Mann-Whitney *t*-test or a nonparametric, one-way Kruskal-Wallis ANOVA followed by Dunn's *post hoc* testing were used. Correlation analysis was performed using a nonparametric Spearman correlation (sensitivity analyses were performed), and a linear regression of the data is displayed. All data meet the assumptions of the statistical tests used. Within each group there is an estimate of variation, and the variance between groups is similar. For each statistical analysis, appropriate tests were selected based on whether the data was normally distributed and whether multiple comparisons were made. Results were considered significant at $P \leq 0.05$. Statistical analyses were performed using Prism version 5.0a (GraphPad Software).

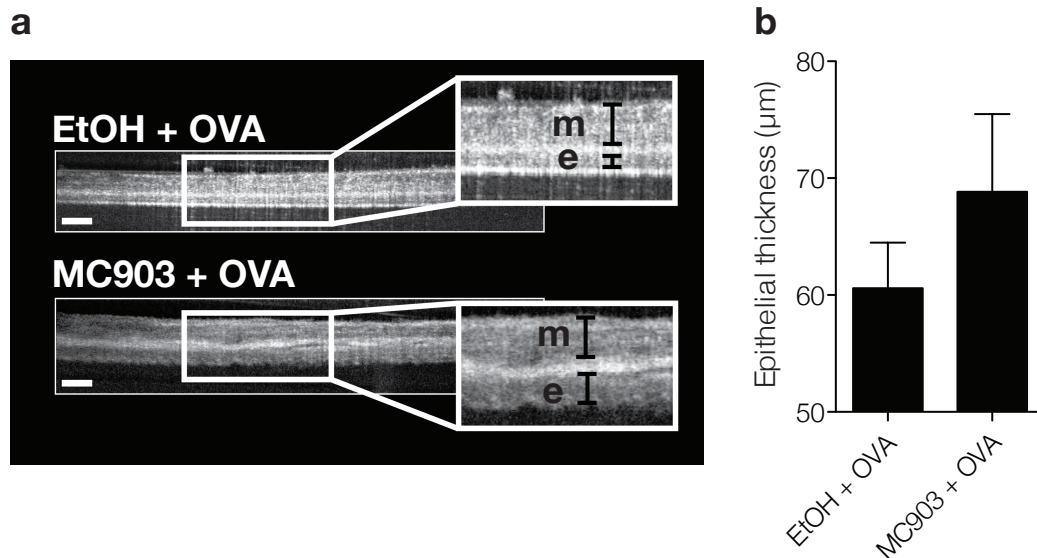
61. Zhang, Z. *et al.* Thymic stromal lymphopoietin overproduced by keratinocytes in mouse skin aggravates experimental asthma. *Proc. Natl. Acad. Sci. USA* **106**, 1536–1541 (2009).

TSLP-elicited basophil responses can mediate the pathogenesis of eosinophilic esophagitis.

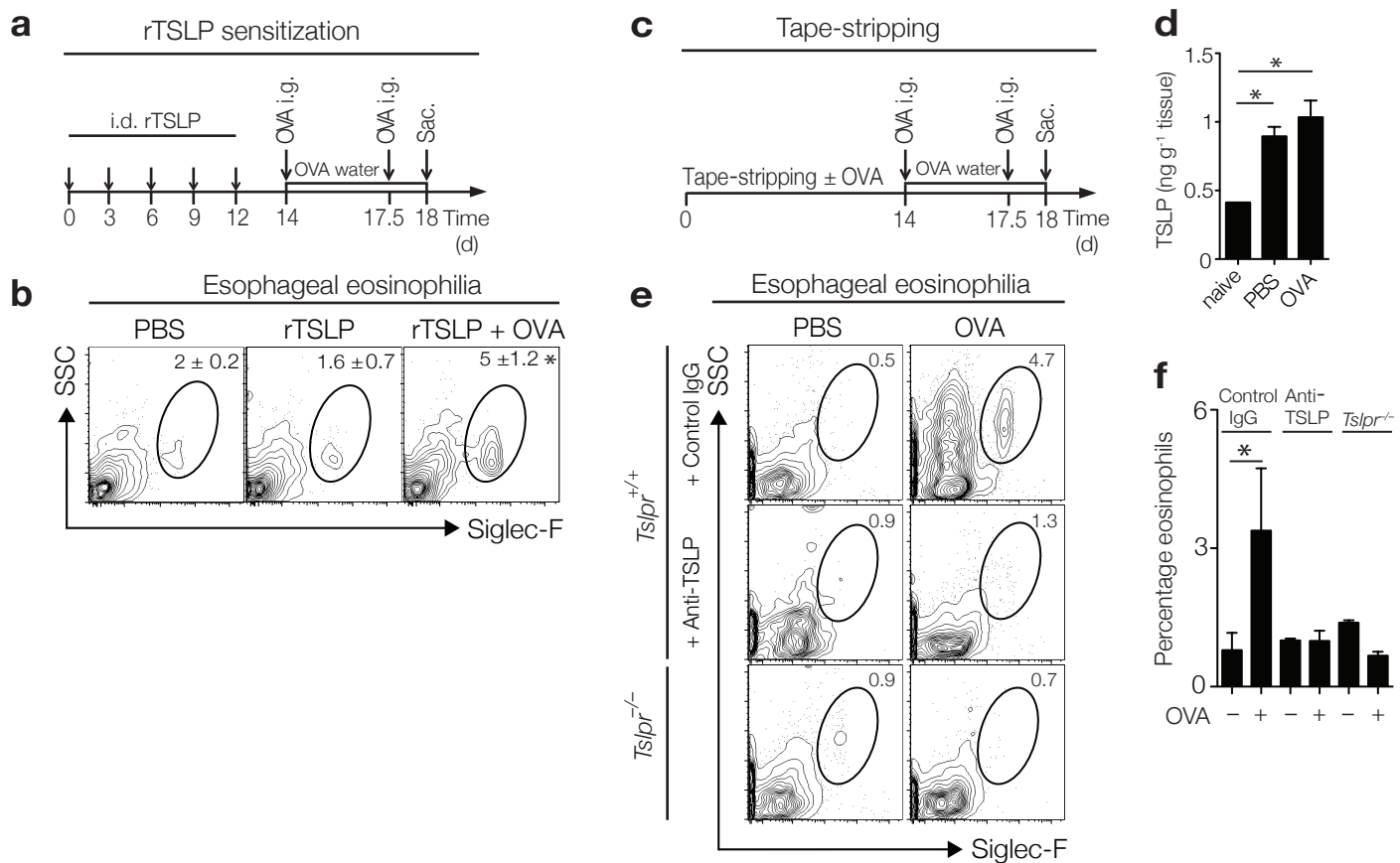
Mario Noti, Elia D. Tait Wojno, Brian S. Kim, Mark C. Siracusa, Paul R. Giacomini, Meera G. Nair, Alain J. Benitez, Kathryn R. Ruymann, Amanda B. Muir, David A. Hill, Kudakwashe R. Chikwava, Amin E. Moghaddam, Quentin J. Sattentau, Aneesh Alex, Chao Zhou, Jennifer H. Yearley, Paul Menard-Katcher, Masato Kubo, Kazushige Obata-Ninomiya, Hajime Karasuyama, Michael R. Comeau, Terri Brown-Whitehorn, Rene de Waal Malefyt, Patrick M. Sleiman, Hakon Hakonarson, Antonella Cianferoni, Gary W. Falk, Mei-Lun Wang, Jonathan M. Spergel, and David Artis



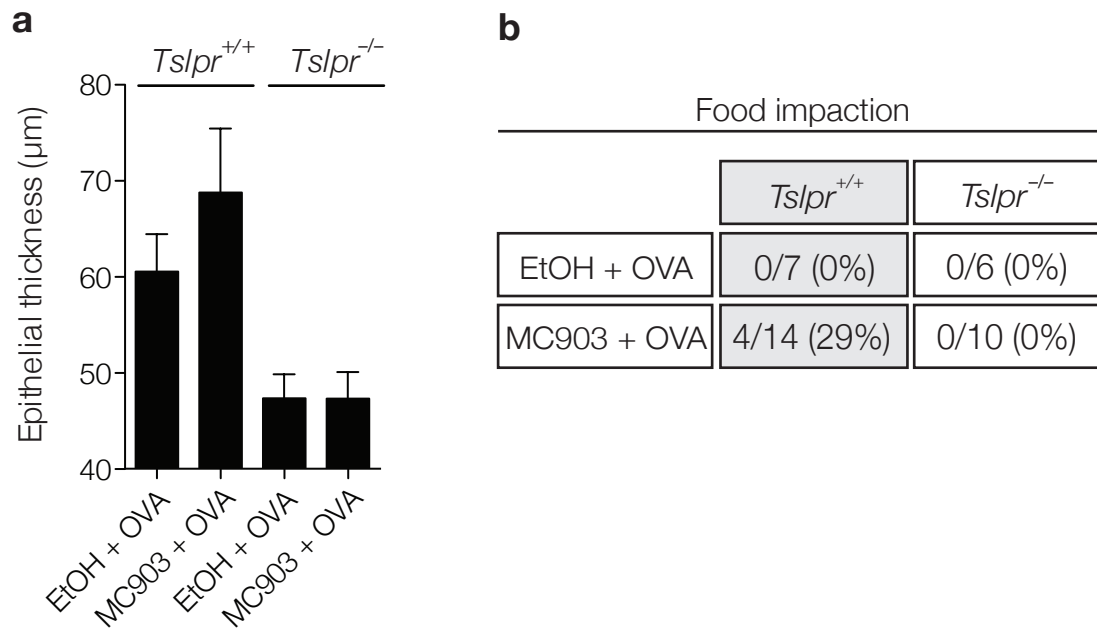
Supplementary Figure 1 Epicutaneous sensitization with peanut antigen and antigen-induced immune responses in the GI tract. **(a)** Histological sections (H & E staining) from the esophagus of WT BALB/c mice. Arrows identify tissue-infiltrating eosinophils. Scale bar: 25 μ m. **(b)** Number of eosinophils per hpf in the esophagus. **(c)** Representative flow cytometry plots showing frequencies of eosinophils in esophageal tissues. Data depicted in **(a–c)** are from one experiment (EtOH + CPE, $n = 3$; MC903, $n = 3$; MC903 + CPE, $n = 4$), and are representative of three independent experiments. Representative flow cytometry plots showing frequencies of eosinophils in **(d)** the stomach and **(e)** small intestine of control (EtOH + OVA) and MC903 + OVA treated WT BALB/c mice. T_H2 cytokines in cell-free supernatants of antigen re-stimulated **(f)** mesenteric lymph nodes (LN) and **(g)** splenocytes of control (EtOH + OVA) and MC903 + OVA treated mice as measured by ELISA. Data depicted in **(d–g)** are from one experiment (EtOH + OVA, $n = 3$; MC903 + OVA, $n = 4$), and are representative of three independent experiments. All parameters in **(a–g)** were assessed 12 h post-final oral antigen challenge. All data depicted in **(a–g)** are from mice challenged twice with OVA. Results are shown as mean \pm sem, and a non-parametric, two-tailed Mann-Whitney t -test or a non-parametric, two-way ANOVA with Bonferroni post-hoc testing were used to determine significance. *, $P \leq 0.05$; **, $P \leq 0.01$; ***, $P \leq 0.001$.



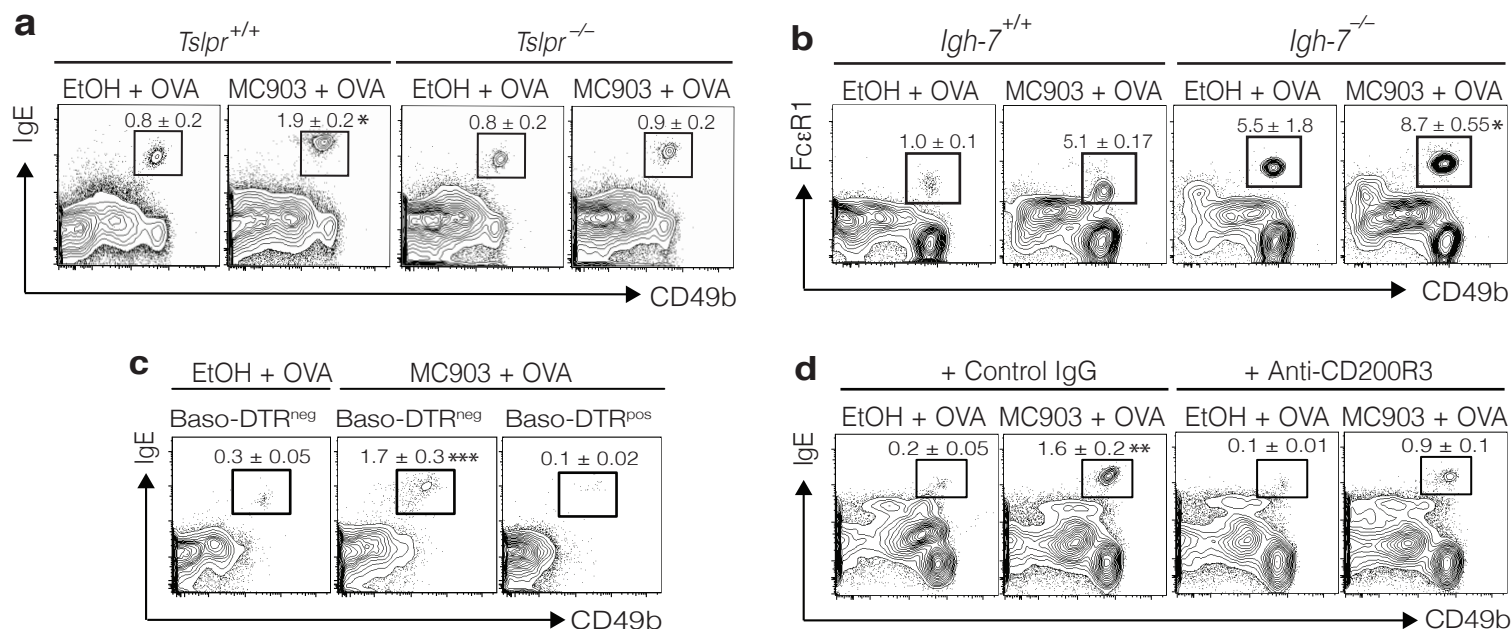
Supplementary Figure 2 OCT analysis reveals epithelial thickening in the esophagus of mice with EoE-like disease. **(a)** Representative OCT images of the esophagus of WT BALB/c mice. Scale bar: 200 μm . **(b)** Quantification of epithelial thickness of the esophagus as measured by OCT. Data depicted in **(a,b)** are from two pooled experiments (EtOH + OVA, $n = 7$; MC903 + OVA, $n = 9$). All parameters were assessed 12 h post-final oral antigen challenge. Data depicted are from mice challenged repeatedly with OVA to induce prolonged inflammation. Results are shown as mean \pm sem.



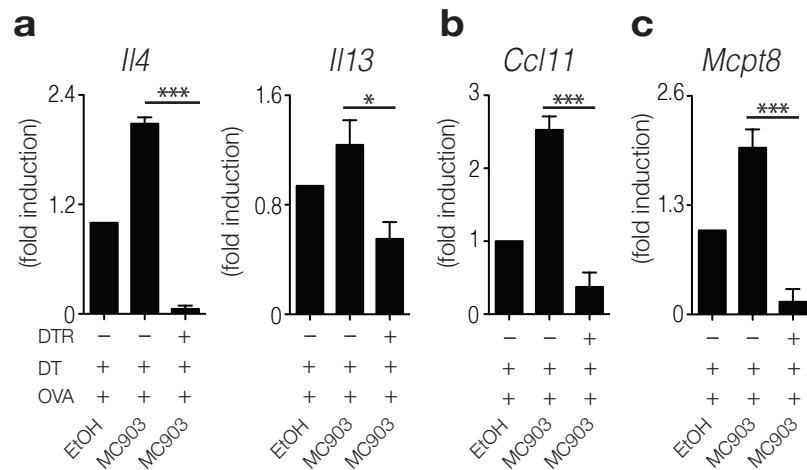
Supplementary Figure 3 Epicutaneous sensitization and oral challenge with a model antigen in the context of elevated TSLP levels results in EoE-like disease. **(a)** Schematic of sensitization in the presence of recombinant TSLP (rTSLP). WT BALB/c mice were injected intradermally (i.d.) on the ears with PBS as control or rTSLP in the presence or absence of OVA. **(b)** Representative flow cytometry plots showing frequencies of eosinophils in esophageal tissues. Data depicted are from one experiment (PBS, $n = 3$; rTSLP, $n = 3$; rTSLP + OVA, $n = 4$), and are representative of three independent experiments. **(c)** Schematic of sensitization on tape-stripped skin. WT BALB/c mice were shaved on the back and sensitized with PBS as control or OVA on tape-stripped skin. **(d)** TSLP expression in cell-free supernatants of overnight-cultured skin (ears) as measured by ELISA. **(e)** Representative flow cytometry plots showing frequencies of eosinophils in esophageal tissues. Data depicted in **(d, e)** are from one experiment (*Tslpr*^{+/+} PBS + IgG, $n = 3$; *Tslpr*^{+/+} OVA + IgG, $n = 3$; *Tslpr*^{+/+} PBS + anti-TSLP mAb, $n = 3$; *Tslpr*^{+/+} OVA + anti-TSLP mAb, $n = 3$; *Tslpr*^{-/-} PBS, $n = 3$; *Tslpr*^{-/-} OVA, $n = 3$), and are representative of three independent experiments. **(f)** Frequencies of eosinophils in esophageal tissues as measured by flow cytometry. Data depicted are from two pooled experiments (*Tslpr*^{+/+} PBS + IgG, $n = 5$; *Tslpr*^{+/+} OVA + IgG, $n = 6$; *Tslpr*^{+/+} PBS + anti-TSLP mAb, $n = 5$; *Tslpr*^{+/+} OVA + anti-TSLP mAb, $n = 7$; *Tslpr*^{-/-} PBS, $n = 5$; *Tslpr*^{-/-} OVA, $n = 6$). All parameters were assessed 12 h post-final oral antigen challenge. Data depicted are from mice challenged twice with OVA. Results are shown as mean ± sem, and a non-parametric, one-way Kruskal-Wallis ANOVA with Dunn's post-hoc testing or a non-parametric, two-way ANOVA with Bonferroni post-hoc testing were used to determine significance. *, $P \leq 0.05$.



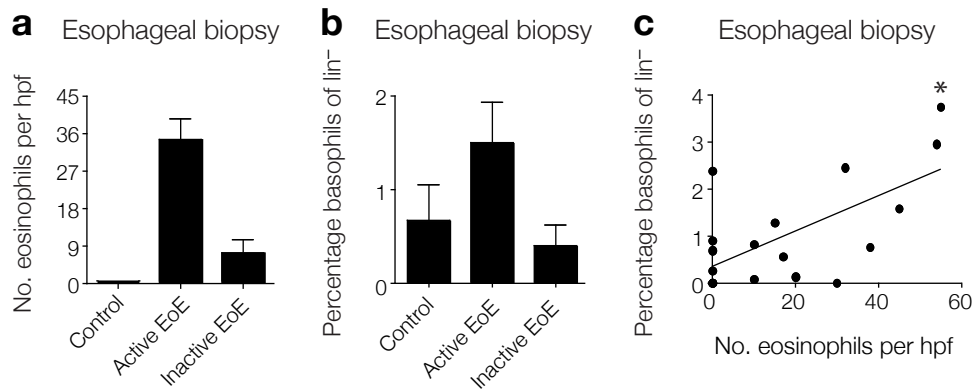
Supplementary Figure 4 Reduced epithelial thickening of the esophagus and absence of food impaction in *Tslpr*^{-/-} mice. **(a)** Quantification of epithelial thickness of the esophagus of BALB/c *Tslpr*^{+/+} and BALB/c *Tslpr*^{-/-} mice as measured by OCT. Data depicted are from one experiment (EtOH + OVA *Tslpr*^{+/+}, *n* = 6; MC903 + OVA *Tslpr*^{+/+}, *n* = 9; EtOH + OVA *Tslpr*^{-/-}, *n* = 4; MC903 + OVA *Tslpr*^{-/-}, *n* = 6). **(b)** Table summarizing the incidence of food impaction in the esophagus. Data depicted are from two pooled experiments (EtOH + OVA *Tslpr*^{+/+}, *n* = 7; MC903 + OVA *Tslpr*^{+/+}, *n* = 14; EtOH + OVA *Tslpr*^{-/-}, *n* = 6; MC903 + OVA *Tslpr*^{-/-}, *n* = 10). All parameters were assessed 12 h post-final oral antigen challenge. Data depicted are from mice challenged repeatedly with OVA to induce extended inflammation. Results are shown as mean ± sem.



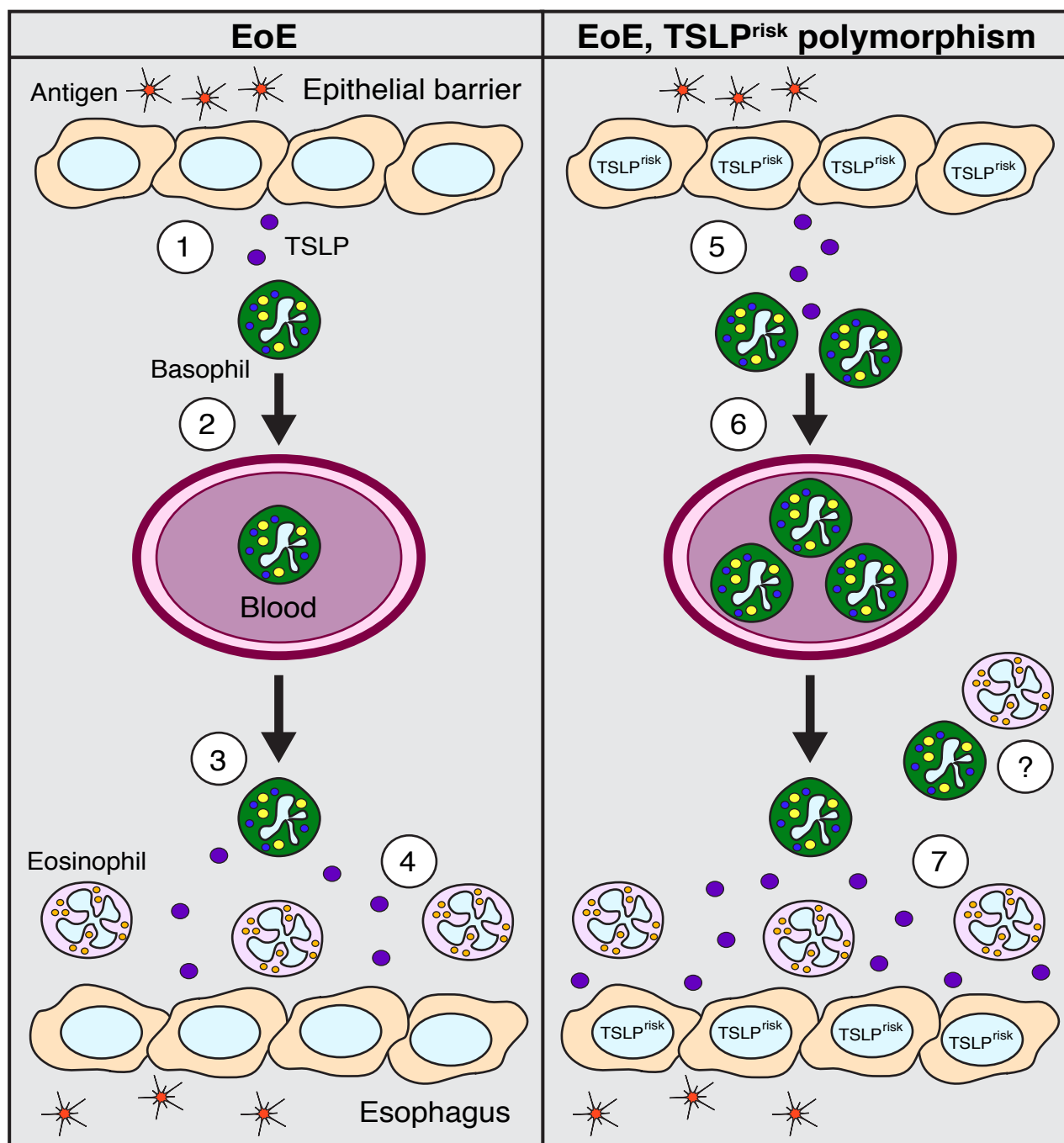
Supplementary Figure 5 Peripheral basophil responses. **(a)** Representative flow cytometry plots showing frequencies of basophils in the periphery of BALB/c *Tslpr*^{+/+} and BALB/c *Tslpr*^{-/-} mice. Data depicted are from one experiment (EtOH + OVA *Tslpr*^{+/+}, *n* = 3; MC903 + OVA *Tslpr*^{+/+}, *n* = 3; EtOH + OVA *Tslpr*^{-/-}, *n* = 3; MC903 + OVA *Tslpr*^{-/-}, *n* = 4), and are representative of three or more independent experiments. For statistical analysis, MC903 + OVA *Tslpr*^{+/+} and MC903 + OVA *Tslpr*^{-/-} are compared. **(b)** Representative flow cytometry plots showing frequencies of basophils in the periphery of BALB/c *Igh*-7^{+/+} and BALB/c *Igh*-7^{-/-} mice. Data depicted are from one experiment (EtOH+OVA *Igh*-7^{+/+}, *n*=3; MC903+OVA *Igh*-7^{+/+}, *n*=3; EtOH+OVA *Igh*-7^{-/-}, *n* = 3; MC903 + OVA *Igh*-7^{-/-}, *n* = 4), and are representative of three independent experiments. For statistical analysis, MC903 + OVA *Igh*-7^{+/+} and MC903 + OVA *Igh*-7^{-/-} are compared. **(c)** Representative flow cytometry plots showing frequencies of basophils in the periphery of C57BL/6 Baso-DTR^{neg} and C57BL/6 Baso-DTR^{pos} mice. Data depicted are from one experiment (EtOH + OVA Baso-DTR^{neg}, *n* = 3; MC903 + OVA Baso-DTR^{neg}, *n* = 3; MC903 + OVA Baso-DTR^{pos}, *n* = 4), and are representative of three independent experiments. For statistical analysis, MC903 + OVA Baso-DTR^{neg} and MC903 + OVA Baso-DTR^{pos} are compared. **(d)** Representative flow cytometry plots showing frequencies of basophils in the periphery of control antibody or anti-CD200R3 mAb treated WT BALB/c mice. Data depicted are from one experiment (EtOH + OVA + IgG, *n* = 3; MC903 + OVA + IgG, *n* = 3; EtOH + OVA + anti-CD200R3 mAb, *n* = 3; MC903 + OVA + anti-CD200R3 mAb, *n* = 4), and are representative of three independent experiments. For statistical analysis, MC903 + OVA + IgG or MC903 + OVA + anti-CD200R3 mAb are compared. All parameters were assessed 12 h post-final oral antigen challenge. All data depicted are from mice challenged twice with OVA. Results are shown as mean ± sem, and a non-parametric, two-way ANOVA with Bonferroni post-hoc testing was used to determine significance. *, *P* ≤ 0.05; **, *P* ≤ 0.01; ***, *P* ≤ 0.001.



Supplementary Figure 6 Reduced inflammatory responses in the esophagus of mice with EoE-like disease depleted of basophils. mRNA expression levels of **(a)** T_H2 cytokines (*Il4*, *Il13*), **(b)** *Ccl11*, and **(c)** the basophil-specific protease *Mcpt8* in the esophagus of C57BL/6 Baso-DTR^{neg} and C57BL/6 Baso-DTR^{pos} mice. Data depicted in **(a–c)** are from one experiment (EtOH + OVA Baso-DTR^{neg}, $n = 3$; MC903 + OVA Baso-DTR^{neg}, $n = 4$; MC903 + OVA Baso-DTR^{pos}, $n = 4$), and are representative of two independent experiments. All parameters were assessed 12 h post-final oral antigen challenge. Data depicted are from mice challenged twice with OVA. Results are shown as mean \pm sem, and a non-parametric, one-way Kruskal-Wallis ANOVA with Dunn's post-hoc testing was used to determine significance. *, $P \leq 0.05$; ***, $P \leq 0.001$.



Supplementary Figure 7 Elevated basophil responses in adult subjects with EoE positively correlate with esophageal eosinophil counts. **(a)** Number of eosinophils per hpf in adult esophageal biopsy tissue sections were quantified for control subjects ($n = 6$), subjects with active EoE ($n = 9$), and subjects with inactive EoE ($n = 3$). **(b)** Frequencies of basophils in the lin⁻ compartment (see Methods) in esophageal biopsies from control subjects ($n = 6$), active subjects with EoE ($n = 9$), and inactive subjects with EoE ($n = 3$). **(c)** Correlation of frequencies of basophils in the lin⁻ compartment in adult esophageal biopsies and the number of eosinophils per hpf observed histologically ($n = 18$) (Spearman $r = 0.5282$). Data are shown as mean \pm sem. Correlation analysis was performed using a non-parametric Spearman correlation (sensitivity analyses were performed), and a linear regression of the data is displayed. *, $P \leq 0.05$.



Supplementary Figure 8 Proposed model of the relationship between a gain-of-function *TSLP* polymorphism (*TSLP^{risk}*), peripheral basophil responses, and the development of EoE in humans. In humans that do not carry the *TSLP^{risk}* polymorphism, exposure to antigens at epithelial barriers may induce TSLP expression which can result in local (1) and systemic (2) TSLP-elicited basophil responses. Encounter with the antigen in the esophagus may promote additional TSLP expression and mobilization of TSLP-elicited basophil populations from the blood to esophageal tissue (3). The studies presented here suggest that TSLP-elicited basophils and their products contribute to esophageal inflammation, including the accumulation of eosinophils, and other immune cells, such as T cells, B cells, and mast cells (not depicted) (4). In humans that carry the *TSLP^{risk}* polymorphism, exposure to antigens at epithelial barriers is more likely to result in enhanced TSLP expression (5) associated with TSLP-elicited peripheral basophilia (6), which together increase the likelihood of, but are not required for, developing EoE in the context of antigen-induced TSLP over-expression in the esophagus (7). It is currently unknown whether the *TSLP^{risk}* polymorphism and peripheral basophilia also promote increased accumulation of basophils and eosinophils in the esophagus in the context of EoE.